

C-8

CIC-14 REPORT COLLECTION  
REPRODUCTION  
COPY

LA-2043

**LOS ALAMOS SCIENTIFIC LABORATORY**  
**OF THE UNIVERSITY OF CALIFORNIA • LOS ALAMOS NEW MEXICO**

**THE PROPERTIES OF PHOSPHORIC ACID  
SOLUTIONS OF URANIUM  
AS FUELS FOR HOMOGENEOUS REACTORS**

LOS ALAMOS NATIONAL LABORATORY



3 9338 00320 7825

#### LEGAL NOTICE

This report was prepared as an account of Government sponsored work. Neither the United States, nor the Commission, nor any person acting on behalf of the Commission:

A. Makes any warranty or representation, express or implied, with respect to the accuracy, completeness, or usefulness of the information contained in this report, or that the use of any information, apparatus, method, or process disclosed in this report may not infringe privately owned rights; or

B. Assumes any liabilities with respect to the use of, or for damages resulting from the use of any information, apparatus, method, or process disclosed in this report.

As used in the above, "person acting on behalf of the Commission" includes any employee or contractor of the Commission to the extent that such employee or contractor prepares, handles or distributes, or provides access to, any information pursuant to his employment or contract with the Commission.

Printed in USA. Price 40 cents. Available from the  
Office of Technical Services  
U. S. Department of Commerce  
Washington 25, D. C.

LA-2043  
CHEMISTRY  
(Distributed according to  
TID-4500, 11th edition)

**LOS ALAMOS SCIENTIFIC LABORATORY**  
**OF THE UNIVERSITY OF CALIFORNIA    LOS ALAMOS    NEW MEXICO**

**REPORT WRITTEN: March 6, 1956**

**REPORT DISTRIBUTED: NOV 27 1956**

**THE PROPERTIES OF PHOSPHORIC ACID  
SOLUTIONS OF URANIUM  
AS FUELS FOR HOMOGENEOUS REACTORS**

Work done by:

R. M. Bidwell  
H. M. Busey  
R. A. Clark  
S. H. Cox  
L. A. Geoffrion  
R. P. Hammond  
G. E. Meadows  
B. J. Melton  
R. H. Perkins  
J. R. Phillips  
M. G. Redman  
J. D. Rogers  
A. Sesonske  
L. R. Sitney  
E. O. Swickard  
B. J. Thamer  
W. R. Wykoff  
J. B. Zorn

Report written by:

B. J. Thamer



**Contract W-7405-ENG. 36 with the U. S. Atomic Energy Commission**



## ABSTRACT

Data secured up to March 1956 are given on the properties of aqueous phosphoric acid solutions of uranium that might be suitable for use in homogeneous reactors. Included is information on solubility, radiation stability, vapor pressure, thermal expansion of the liquid phase, and corrosion. Sufficient uranium solubility in the system  $\text{UO}_3\text{-H}_3\text{PO}_4\text{-H}_2\text{O}$  is readily obtainable with as little as 2 or 3 M phosphoric acid. Adequate uranium solubility in the system  $\text{UO}_2\text{-H}_3\text{PO}_4\text{-H}_2\text{O}$  requires the use of concentrated phosphoric acid, but these solutions have the advantages of low vapor pressure and low equilibrium pressure of radiolytic hydrogen and oxygen. A brief discussion is given of feasible methods of reprocessing phosphate fuel solutions with the use of only inorganic reagents.

## ACKNOWLEDGEMENT

The writer wishes to thank D. B. Hall, R. P. Hammond, and R. M. Bidwell for their suggestions concerning the content and form of this report.



## CONTENTS

	Page
Abstract .....	3
Chapter 1. The System $\text{UO}_3\text{-H}_3\text{PO}_4\text{-H}_2\text{O}$ .....	9
1.1 Solubility .....	9
1.2 Radiation Stability .....	13
1.3 Vapor Pressure .....	16
1.4 Thermal Expansion of the Liquid Phase .....	16
1.5 Corrosion .....	22
Chapter 2. The System $\text{UO}_2\text{-H}_3\text{PO}_4\text{-H}_2\text{O}$ .....	30
2.1 Solubility .....	30
2.2 Radiation Stability .....	30
2.3 Vapor Pressure .....	33
2.4 Thermal Expansion of the Liquid Phase .....	33
2.5 Corrosion .....	37
Chapter 3. Reprocessing Methods .....	39
Appendix A .....	42
Appendix B .....	46
References .....	57

## TABLES

Table 1.1	Solubility Data Obtained Upon Equilibrating Excess Solid $(\text{UO}_2)_3(\text{PO}_4)_2 \cdot 4\text{H}_2\text{O}$ with a Solution of Initially 0.30 M $\text{UO}_3$ Dissolved in 2.0 M $\text{H}_3\text{PO}_4$ .....	10
-----------	--	----

# CONTENTS (cont'd)

	Page
Table 1.2	
Solubility Data Obtained Upon Equilibrating Excess	
Solid $(\text{UO}_2)_3(\text{PO}_4)_2 \cdot 4\text{H}_2\text{O}$ with a Solution of Ini-	
tially 0.3 to 0.5 M $\text{UO}_3$ Dissolved in 2.9 to 3.2 M	
$\text{H}_3\text{PO}_4$ .....	11
Table 1.3	
The Density at 25° C. of Solutions of $\text{UO}_3$ in $\text{H}_3\text{PO}_4$ ..	12
Table 1.4	
The Solubility of $\text{Cu}^{+2}$ in Two $\text{UO}_3$ - $\text{H}_3\text{PO}_4$ Solutions ...	27
Table 2.1	
Solubility Data in the System $\text{UO}_2$ - $\text{H}_3\text{PO}_4$ - $\text{H}_2\text{O}$ .....	31
Table 2.2	
Description of Solid Phases .....	32
Table 2.3	
The Density at 25° C. of Solutions of $\text{UO}_2$ in $\text{H}_3\text{PO}_4$ ..	32
Table A.1	
Solubility Data Obtained Upon Equilibrating Excess	
Solid $(\text{UO}_2)_3(\text{PO}_4)_2 \cdot 4\text{H}_2\text{O}$ with a Solution of Ini-	
tially 0.3 M $\text{UO}_3$ Dissolved in 1.7 M $\text{H}_3\text{PO}_4$ + 0.3 M	
$\text{NaH}_2\text{PO}_4$ .....	44
Table A.2	
Solubility Data Obtained Upon Equilibrating Excess	
Solid $(\text{UO}_2)_3(\text{PO}_4)_2 \cdot 4\text{H}_2\text{O}$ with a Solution of Ini-	
tially 0.316 M $\text{UO}_2(\text{NO}_3)_2$ Dissolved in 2.07 M $\text{H}_3\text{PO}_4$ ..	45
Table A.3	
Composition of Solid Phase After Equilibrating	
$(\text{UO}_2)_3(\text{PO}_4)_2 \cdot 4\text{H}_2\text{O}$ at 150° C. with Initially 0.316 M	
$\text{UO}_2(\text{NO}_3)_2$ in 2.07 M $\text{H}_3\text{PO}_4$ .....	45
Table B.1	
Corrosion Tests with a Solution of 0.77 M $\text{UO}_2$ + 0.03	
M $\text{UO}_3$ Dissolved in 14.1 M $\text{H}_3\text{PO}_4$ + 0.20 M $\text{H}_3\text{PO}_3$ .....	47



## CONTENTS (cont'd)

	Page
Table B.2	Corrosion Tests at 430° C. for Four Days, Each
	Solution Containing 0.20 M $\text{H}_3\text{PO}_3$ ..... 48
Table B.3	Corrosion Tests at 430° C. for 25 Days in 14.5 M
	$\text{H}_3\text{PO}_4$ + 0.20 M $\text{H}_3\text{PO}_3$ ..... 49
Table B.4	Pinhole and Average Corrosion Rates with Gold-Plated
	Silver ..... 50
Table B.5	Pinhole and Average Corrosion Rates with Graphite-
	Clad Silver ..... 51
Table B.6	The Effect of Hydrogen on the Corrosion of Bare
	Silver ..... 53
Table B.7	Corrosion Tests in the Absence of Galvanic Couples ... 53

## ILLUSTRATIONS

Figure 1.1	Recombination Rates vs. Temperature in the Absence of
	Dissolved Copper ..... 15
Figure 1.2	Representative Vapor Pressures ..... 17
Figure 1.3	Behavior of Liquid Volume vs. Temperature for 3 to 4 M
	$\text{H}_3\text{PO}_4$ ..... 18
Figure 1.4	Behavior of Liquid Volume vs. Temperature at Various
	Concentrations of $\text{H}_3\text{PO}_4$ ..... 19
Figure 1.5	Behavior of Liquid Volume vs. Temperature for 7.5 M
	$\text{H}_3\text{PO}_4$ ..... 20

# CONTENTS (cont'd)

	Page
Figure 1.6	Temperature of Filling of Container vs. Initial Charge ..... 23
Figure 1.7	Compressibility of Liquid Phase at Elevated Temperatures ..... 24
Figure 1.8	The Corrosion Rate of Type 347 Stainless Steel vs. Temperature in $H_3PO_4$ Solutions of $UO_3$ ..... 25
Figure 2.1	Vapor Pressures vs. Temperature ..... 34
Figure 2.2	Vapor Pressures vs. $H_3PO_4$ Concentration ..... 35
Figure 2.3	Behavior of Liquid Volume vs. Temperature for Concentrated $H_3PO_4$ Solutions ..... 36
Figure B.1	Corrosion Rate vs. Temperature for Bare Silver ..... 55

## Chapter 1

### The System $\text{UO}_3\text{-H}_3\text{PO}_4\text{-H}_2\text{O}$

#### 1.1 Solubility

The solubility of the hexavalent uranium at high temperatures was determined with the constituents contained in closed, high-pressure equipment from which filtered samples of the liquid phase could be withdrawn as desired. The design and operation of the pressure bombs and associated equipment have been described by R. M. Bidwell, W. R. Wykoff, B. J. Thamer, and C. D. Ross.<sup>1,2</sup> The temperature control was within  $1^\circ\text{C}$ . With an excess of solid present, phase equilibrium was indicated when several successive samples of the filtered liquid phase taken over a period of several hundred hours showed the same composition by analysis.

The solubilities that were obtainable when  $\text{UO}_3$  was dissolved in nominally 2 or 3 M phosphoric acid have been given in Tables 1.1 and 1.2, respectively. The density data and formula from which the molalities were calculated have been included in Table 1.3. The solid phase was the  $(\text{UO}_2)_3(\text{PO}_4)_2 \cdot 4\text{H}_2\text{O}$  described by W. W. Harris and R. H. Scott<sup>3</sup> except that a small amount of an orthorhombic modification<sup>4,5</sup> of the same compound sometimes was present also. The increased uranium solubility at the higher phosphoric acid concentrations is largely attributable to the complexing action of the phosphoric acid. In Appendix A are shown the effects on the uranium solubility of neutralizing part of

Table 1.1

Solubility Data Obtained Upon Equilibrating Excess Solid  
 $(\text{UO}_2)_3(\text{PO}_4)_2 \cdot 4\text{H}_2\text{O}$  with a Solution of Initially 0.30 M  $\text{UO}_3$   
 Dissolved in 2.0 M  $\text{H}_3\text{PO}_4$

(Equilibrium Solid Phase:  $(\text{UO}_2)_3(\text{PO}_4)_2 \cdot 4\text{H}_2\text{O}$ )

Temperature, °C.	Analytical Molarities		Molalities		Refs.
	U	Total Phosphate	U	Total Phosphate	
25	0.34 <sup>a</sup>	2.00	0.38	2.21	
161	0.257	1.90	0.285	2.11	4,6
199	0.224	1.91	0.248	2.12	4,6
256	0.201	1.76	0.221	1.93	4,6
267	0.203	1.88	0.224	2.08	6
274	0.195	1.91	0.216	2.11	6
298	0.198	1.95	0.220	2.16	6
330	0.258	2.24	0.291	2.53	6
354	0.308	2.43	0.352	2.77	--
355.5	0.229	2.12	0.257	2.38	6
380	0.592	2.97	0.703	3.53	6
O. H. Day <u>et al.</u> , ORNL-1116:					
250	0.25	2.1	0.28	2.35	7
W. L. Marshall <u>et al.</u> , ORNL-1121 (interpolated):					
250	0.15	2.00	0.17	2.22	8

<sup>a</sup>Taken from the data of J. M. Schreyer and C. F. Baes, Jr.,<sup>9</sup> at 25° C., at which temperature the equilibrium solid phase is  $\text{UO}_2\text{HPO}_4 \cdot 4\text{H}_2\text{O}$ .

Table 1.2

Solubility Data Obtained Upon Equilibrating Excess Solid  
 $(\text{UO}_2)_3(\text{PO}_4)_2 \cdot 4\text{H}_2\text{O}$  with a Solution of Initially 0.3 to 0.5 M  $\text{UO}_3$   
 Dissolved in 2.9 to 3.2 M  $\text{H}_3\text{PO}_4$

(Equilibrium Solid Phase:  $(\text{UO}_2)_3(\text{PO}_4)_2 \cdot 4\text{H}_2\text{O}$ )

Temperature, °C.	Analytical Molarities		Molalities		Refs.
	U	Total Phosphate	U	Total Phosphate	
25	0.62 <sup>a</sup>	3.00	0.74	3.57	
200	0.559	3.12	0.669	3.73	6
250	0.601	3.40	0.731	4.14	6
291	0.561	3.29	0.677	3.97	4,6
O. H. Day <u>et al.</u> , ORNL-1116:					
250	0.60	3.1	0.72	3.7	7
W. L. Marshall <u>et al.</u> , ORNL-1121 (interpolated):					
250	0.29	3.00	0.34	3.53	8

<sup>a</sup>Taken from the data of J. M. Schreyer and C. F. Baes, Jr.,<sup>9</sup> at 25° C., at which temperature the equilibrium solid phase is  $\text{UO}_2\text{HPO}_4 \cdot 4\text{H}_2\text{O}$ .

Table 1.3

The Density at 25° C. of Solutions of  $\text{UO}_3$  in  $\text{H}_3\text{PO}_4$ 

Solution Composition (molarities)	Density, g/ml at 25° C.
0.314 M $\text{UO}_3$ in 1.91 M $\text{H}_3\text{PO}_4$	1.1720
0.335 M $\text{UO}_3$ in 1.95 M $\text{H}_3\text{PO}_4$	1.1886
0.195 M $\text{UO}_3$ in 2.94 M $\text{H}_3\text{PO}_4$	1.1998
0.248 M $\text{UO}_3$ in 2.96 M $\text{H}_3\text{PO}_4$	1.2125
0.291 M $\text{UO}_3$ in 2.96 M $\text{H}_3\text{PO}_4$	1.2252
0.341 M $\text{UO}_3$ in 2.96 M $\text{H}_3\text{PO}_4$	1.2379
0.559 M $\text{UO}_3$ in 6.08 M $\text{H}_3\text{PO}_4$	1.4418
0.467 M $\text{UO}_3$ in 7.38 M $\text{H}_3\text{PO}_4$	1.4805
0.555 M $\text{UO}_3$ in 7.55 M $\text{H}_3\text{PO}_4$	1.5041
0.567 M $\text{UO}_3$ in 7.79 M $\text{H}_3\text{PO}_4$	1.5208
0.647 M $\text{UO}_3$ in 7.49 M $\text{H}_3\text{PO}_4$	1.5280

The above density data in 2 to 3 M  $\text{H}_3\text{PO}_4$  may be represented by the formula  $d = 1.2316 + 0.0518 ([\text{H}_3\text{PO}_4] - 2.96) + 0.255 ([\text{U}] - 0.316)$  where brackets indicate molarities.

the phosphoric acid or substituting  $\text{UO}_2(\text{NO}_3)_2$  for  $\text{UO}_3$ . Any gains in uranium solubility so obtained would appear to be more readily obtainable by simply increasing the concentration of phosphoric acid instead.

If a solution of  $\text{UO}_3$  in concentrated  $\text{H}_3\text{PO}_4$  is heated with an air atmosphere in a closed container, it can be observed that at temperatures of  $200^\circ\text{C}$ . and higher the uranium spontaneously evolves oxygen and is converted to the tetravalent state. The decomposition also is appreciable after a period of several months at room temperature. The decomposition is more rapid and more extensive the higher the phosphoric acid concentration. Such decomposition was prevented in obtaining the data of Tables 1.1, 1.2, A.1, and A.2 by having a pressure of 300 psi of oxygen placed in the bomb before heating was begun. That such a high pressure of oxygen was not necessary has been indicated by the fact that tests at  $430^\circ$ ,  $300^\circ$ , and  $170^\circ\text{C}$ . of several hundred hours' duration at each temperature have shown the thermal stability of a solution of 0.60 M  $\text{UO}_3$  in 7.50 M  $\text{H}_3\text{PO}_4$  over which had been placed 200 psi of oxygen at room temperature. The tests also indicated that the uranium was completely soluble in the latter solution.

## 1.2 Radiation Stability

It has been reported that decomposition of 85%  $\text{H}_3\text{PO}_4$  takes place upon irradiation in a Van de Graaff for 5.5 minutes at an ionization density corresponding to 550 kw/l in a homogeneous reactor.<sup>10</sup> In spite of this, phosphate ion is considered to be adequately stable to reactor radiation.<sup>11</sup> This view is supported by experimental work done

at Oak Ridge National Laboratory. In this experiment a LAPRE I-like type of solution\* was irradiated in a thermal neutron flux of  $1.5 \times 10^{13}$  for ten hours at temperatures from  $260^{\circ}$  to  $390^{\circ}$  C.<sup>12</sup> The solution contained 0.31 M dissolved  $\text{UO}_3$  (approximately 90% enriched) in 2.9 M  $\text{H}_3\text{PO}_4$ . Although the dissolved uranium had a catalytic effect on the recombination of hydrogen and oxygen, a still greater catalytic effect was obtained by incorporating 0.0020 M  $\text{Cu}^{+2}$  in the solution. The solution initially occupied 41% of the volume of its container. The power density which was developed was 60 kw/l, and the solution appeared to be stable under these conditions, although a moderate corrosion of the stainless steel bomb caused some reduction of uranium and copper. It is thought that this stability would extend as well to somewhat higher concentrations and temperatures.

It was found from the above experiments that the pressure of radiolytically produced hydrogen and oxygen at 60 kw/l would be small compared with the vapor pressure of the solution at  $430^{\circ}$  C. This would be true even in the absence of dissolved copper. The equilibrium radiolytic gas pressure is inversely proportional to an experimental recombination rate constant  $k_{\pi}$ , which is the fractional recombination per hour. Figure 1.1 indicates the behavior of  $k_{\pi}$  for a LAPRE I type of solution (lower curve) and a LAPRE II type of solution (upper curve), which type

---

\*The designation "LAPRE" represents "Los Alamos Power Reactor Experiment." LAPRE I is to be operated with 0.5 M enriched  $\text{UO}_3$  in 7.5 M  $\text{H}_3\text{PO}_4$  at  $430^{\circ}$  C., and LAPRE II is to be operated with approximately 0.35 M enriched  $\text{UO}_2$  in 17 M  $\text{H}_3\text{PO}_4$  at  $430^{\circ}$  C.



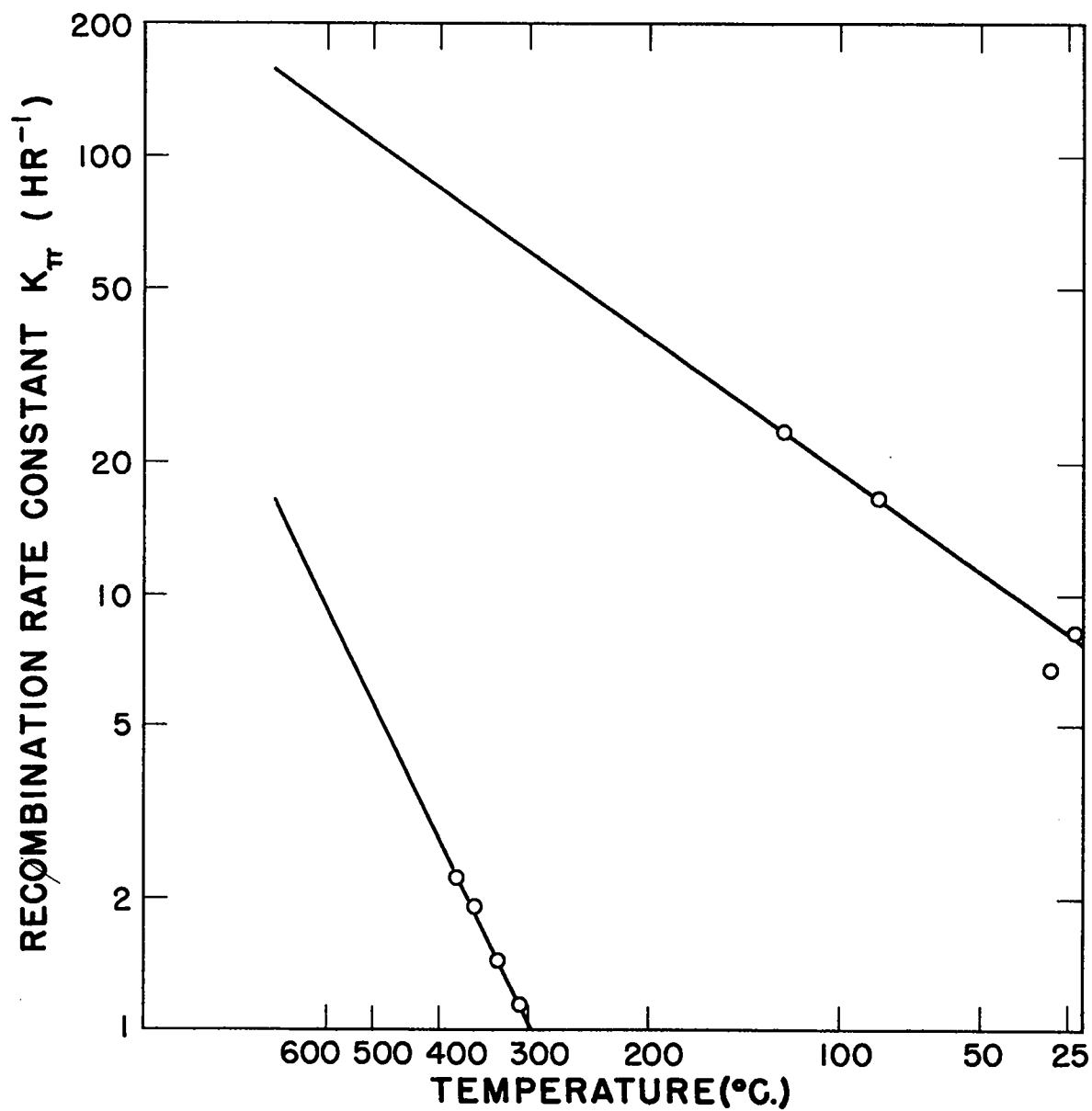


Fig. 1.1 Recombination Rates vs. Temperature in the Absence of Dissolved Copper

Lower curve: 0.31 M  $\text{UO}_3$  in 2.9 M  $\text{H}_3\text{PO}_4$

Upper curve: 0.5 M  $\text{UO}_2$  in 16.5 M  $\text{H}_3\text{PO}_4$

of solution is to be described in Chapter 2. Although  $k_{\pi}$  is much lower for the LAPRE I type of solution than it is for the LAPRE II type, nevertheless, it would be satisfactorily high for LAPRE I operation at 400° C. or above.

### 1.3 Vapor Pressure

Figure 1.2 contains representative vapor-pressure data. Included in the figure for the sake of comparison is the vapor-pressure curve for pure water<sup>13</sup> up to its critical temperature  $T_c = 374^{\circ}$  C. The critical temperatures were not reached for any of the phosphate solutions represented in the figure. The presence of the phosphoric acid appreciably lowers the vapor pressure, but the presence of the uranium appears to raise it slightly.

### 1.4 Thermal Expansion of the Liquid Phase

Measurements of the thermal expansion of the liquid phase with increasing temperature were made with cathetometer measurements on solutions that had been sealed in thick-walled quartz capillaries. The capillaries were held at temperatures uniform to 1° C. in a cylindrical Pyrex heating device that was heated by electrical heating wire wound around its exterior. The curves of Figures 1.3, 1.4, and 1.5 are representative of the data that were obtained. In the instances noted the meniscus disappeared and the uranium as well as the rest of the liquid phase became uniformly distributed throughout the capillary in a single fluid phase. This phenomenon corresponds to passage through the critical temperature of the solution. The data of Figure 1.3 show that at

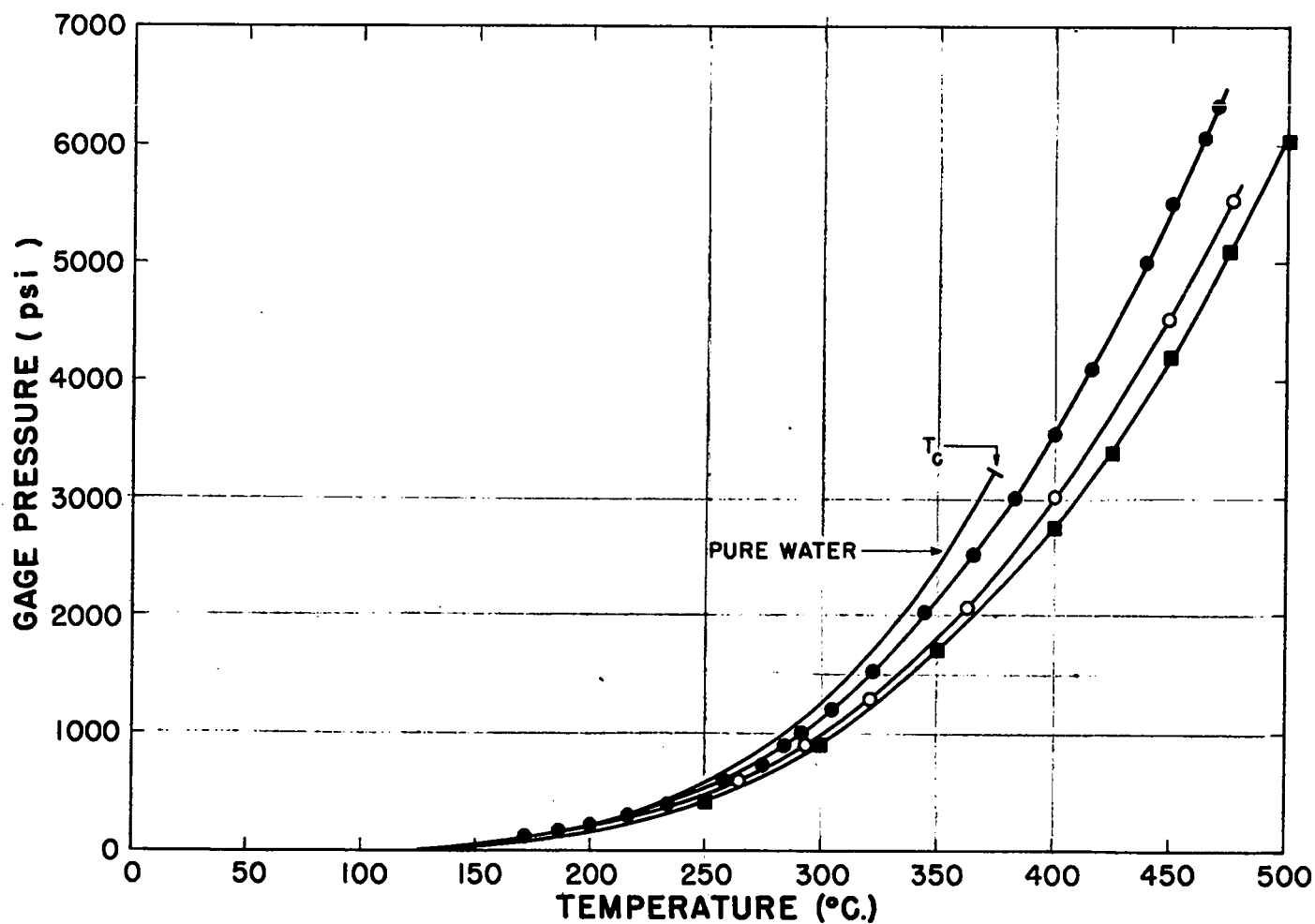


Fig. 1.2 Representative Vapor Pressures

- - 0.764 M  $UO_3$  dissolved in 5.28 M  $H_3PO_4$ , 58% initial degree of filling
- - 0.75 M  $UO_3$  dissolved in 7.50 M  $H_3PO_4$ , 58% initial degree of filling
- - 7.61 M  $H_3PO_4$ , 58% initial degree of filling

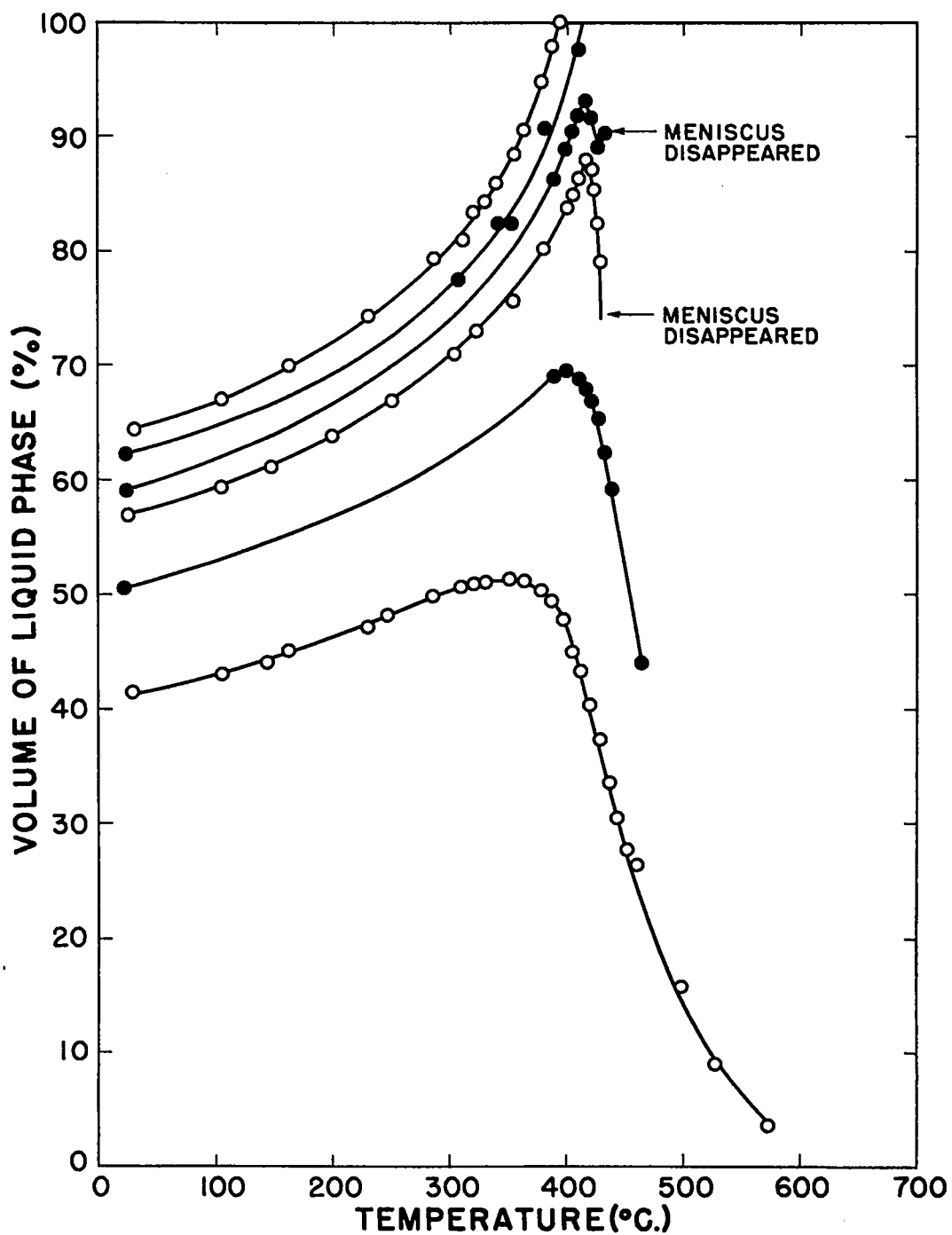


Fig. 1.3 Behavior of Liquid Volume vs. Temperature for 3 to 4 M  $\text{H}_3\text{PO}_4$

○ - 0.31 M  $\text{UO}_3$  in 2.90 M  $\text{H}_3\text{PO}_4$

● - 0.48 M  $\text{UO}_3$  in 4.10 M  $\text{H}_3\text{PO}_4$

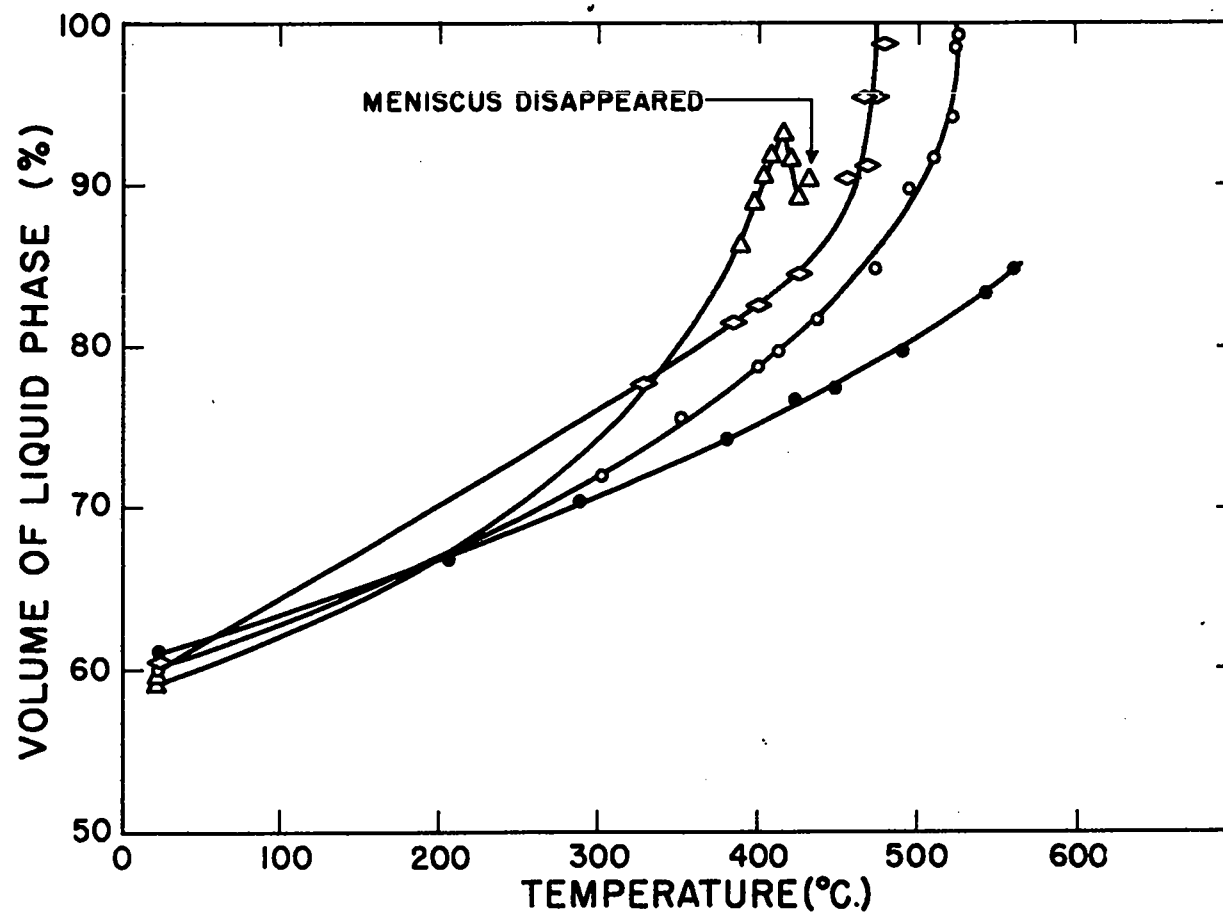


Fig. 1.4 Behavior of Liquid Volume vs. Temperature at Various Concentrations of  $\text{H}_3\text{PO}_4$

- $\Delta$  - 0.48 M  $\text{UO}_3$  in 4.10 M  $\text{H}_3\text{PO}_4$
- $\diamond$  - 0.46 M  $\text{UO}_3$  in 5.61 M  $\text{H}_3\text{PO}_4$
- $\circ$  - 0.49 M  $\text{UO}_3$  in 7.5 M  $\text{H}_3\text{PO}_4$
- $\bullet$  - 0.48 M  $\text{UO}_3$  in 12.7 M  $\text{H}_3\text{PO}_4$

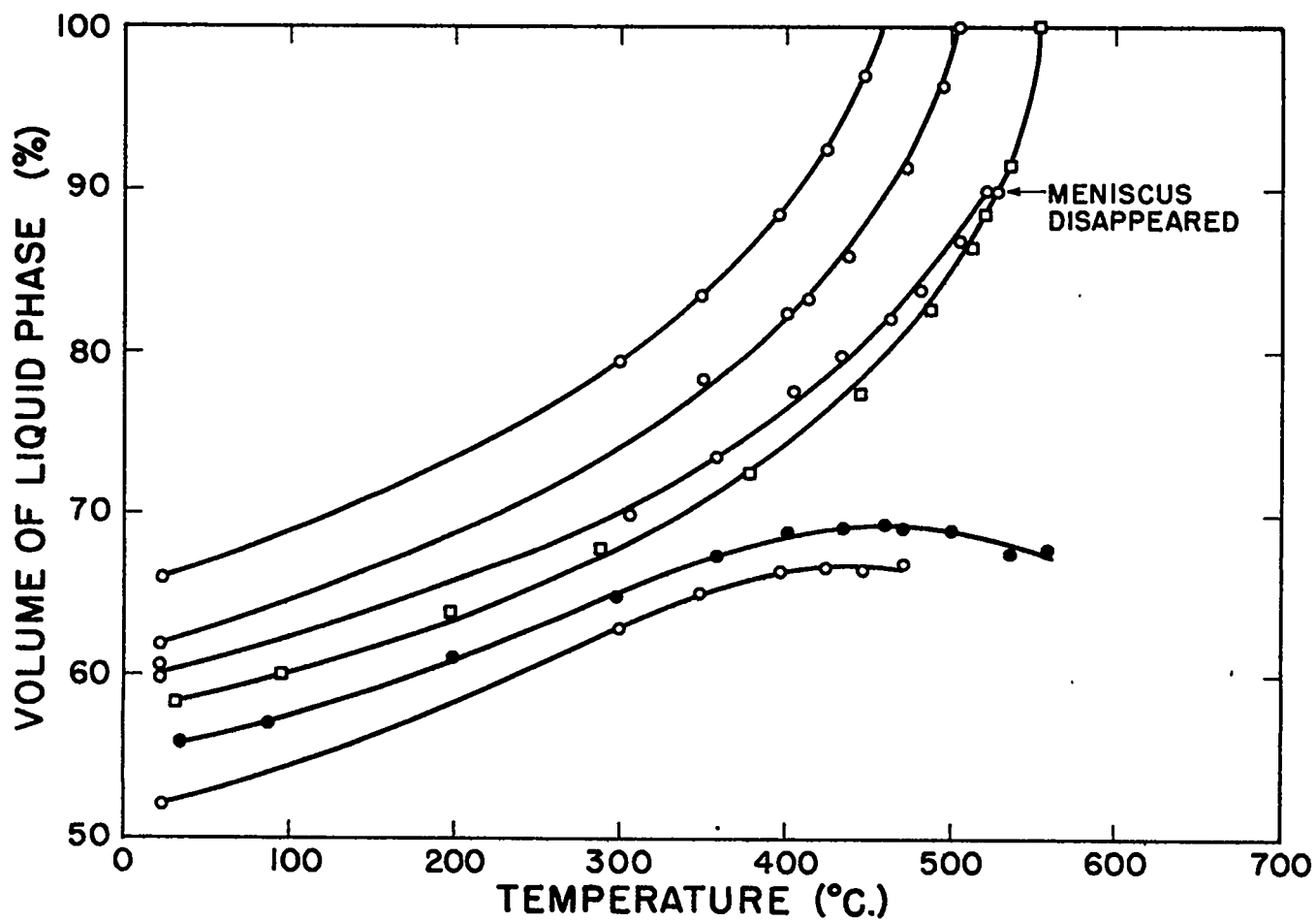


Fig. 1.5 Behavior of Liquid Volume vs. Temperature for 7.5 M  $\text{H}_3\text{PO}_4$

- - 0.49 M  $\text{UO}_3$  in 7.5 M  $\text{H}_3\text{PO}_4$
- - 0.69 M  $\text{UO}_3$  in 7.4 M  $\text{H}_3\text{PO}_4$
- - 7.61 M  $\text{H}_3\text{PO}_4$

3 to 4 M  $\text{H}_3\text{PO}_4$  the disappearance of the meniscus occurs in the neighborhood of  $430^\circ \text{C}$ ., some  $60^\circ$  above the critical point of water. Figure 1.4 illustrates the effect on the volume behavior of varying the  $\text{H}_3\text{PO}_4$  concentration. As the  $\text{H}_3\text{PO}_4$  concentration is increased, the curve becomes flatter, thus decreasing the negative temperature coefficient for a reactor, but also decreasing the control-rod requirements. These considerations, as well as the matter of vapor pressure, make the 7.5 M  $\text{H}_3\text{PO}_4$  concentration of Figure 1.5 more desirable for reactor use above  $400^\circ \text{C}$ . than the 3 to 4 M  $\text{H}_3\text{PO}_4$  of Figure 1.3 if corrosion is not a factor. Figure 1.5 also illustrates how the presence of dissolved uranium tends to cause the meniscus to disappear when it would not disappear in the absence of uranium.

At temperatures above  $400^\circ \text{C}$ ., solutions such as those of Figures 1.3, 1.4, and 1.5 are somewhat compressible, but they nevertheless can cause greatly increased stresses in their containers if they are heated beyond the temperature at which the liquid fills the container. Figure 1.6 provides data on temperatures at which various charges of solutions just fill their containers. (Included in the figure are temperatures at which the meniscus disappeared because such temperatures usually are not far from the ones at which the container otherwise would be filled.) The slopes of the best straight lines through the points show the expected result that the higher the volume of the initial charge the lower is the temperature at which the container fills. Increased concentrations of phosphoric acid raise the temperature

at which the container fills. The data of Figure 1.6 were obtained with air at 1 atm in the gas phase over the initial liquid charge. Figure 1.7 illustrates the compressing effect on the liquid phase at high temperatures that can be caused by an added gas.

### 1.5 Corrosion

The corrosion results to be presented were obtained with one specimen per bomb and an initial degree of filling of solution of 60%. Each bomb was clad with platinum or gold except as noted. There was a maximum temperature difference throughout the bomb that has been measured to be  $10 \pm 3^{\circ}$  C., possibly less below  $300^{\circ}$  C. The nominal temperature at each test was that at the hottest portion of the bomb. Under corrosion conditions the ratio of exposed bomb area to specimen area was in the range of 5 to 10. The bombs were rocked at a rate of 2 cycles a minute. Unless otherwise noted, corrosion rates were computed from changes of weight after any loosely adhering corrosion product had been brushed off.

Corrosion tests at various temperatures were made with specimens of Type 347\* stainless steel. At room temperature or  $50^{\circ}$  C. the corrosion rate with 0.6 M  $\text{UO}_3$  in 7.5 M  $\text{H}_3\text{PO}_4$  was hardly measurable (0.01 mil/year). Figure 1.8 shows representative results that were obtained at higher temperatures with three different phosphoric acid concentrations. The general shape of the curve is similar at any phosphoric acid concentration from 3 M to 7.5 M. The increase in corrosion rate with increasing temperature up to about  $200^{\circ}$  C. is due to the

---

\*17 to 19% Cr, 9 to 12% Ni, 0.08% C max., Nb at least ten times the carbon content.



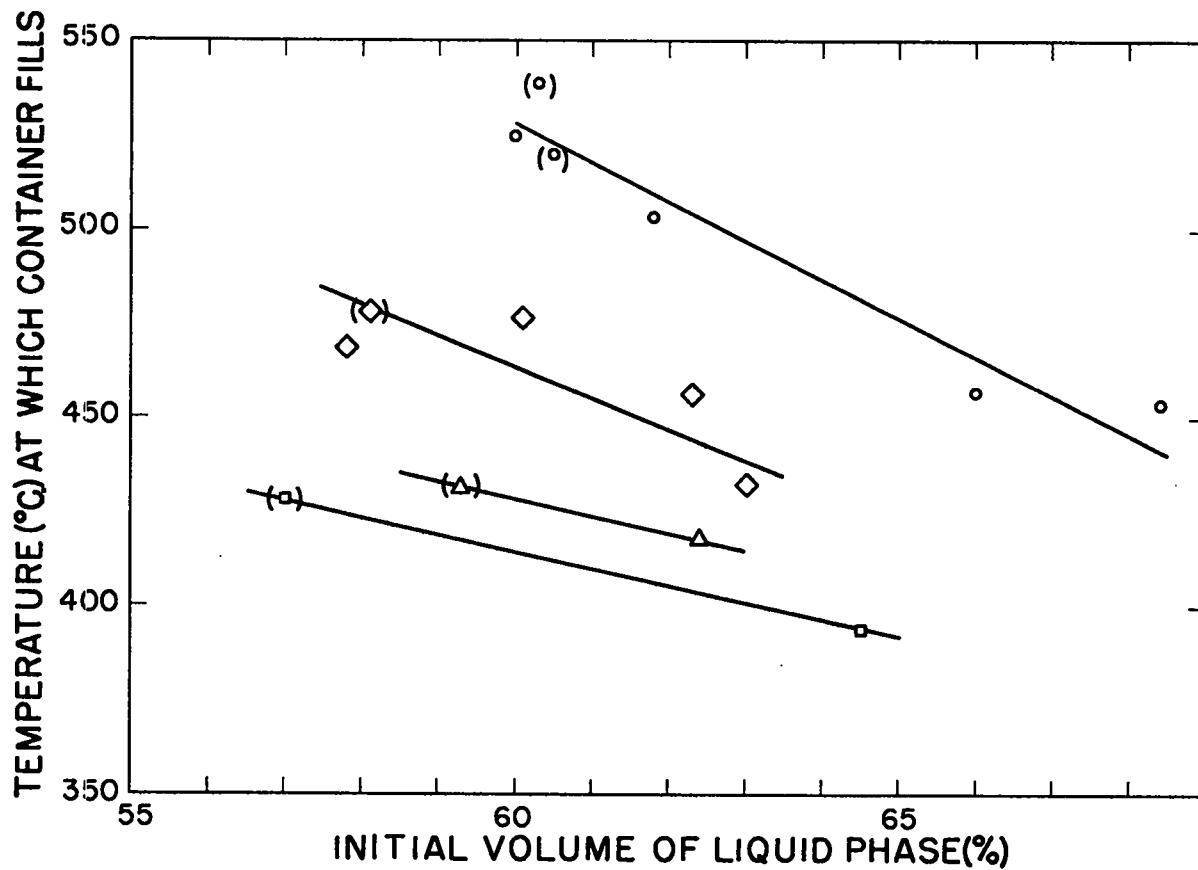


Fig. 1.6 Temperature of Filling of Container vs. Initial Charge

- ( ) - Meniscus disappeared
- ◻ - 0.31 M  $\text{UO}_3$  in 2.90 M  $\text{H}_3\text{PO}_4$
- Δ - 0.48 M  $\text{UO}_3$  in 4.10 M  $\text{H}_3\text{PO}_4$
- ◊ - 0.46 M  $\text{UO}_3$  in 5.61 M  $\text{H}_3\text{PO}_4$
- - 0.49 M  $\text{UO}_3$  in 7.5 M  $\text{H}_3\text{PO}_4$

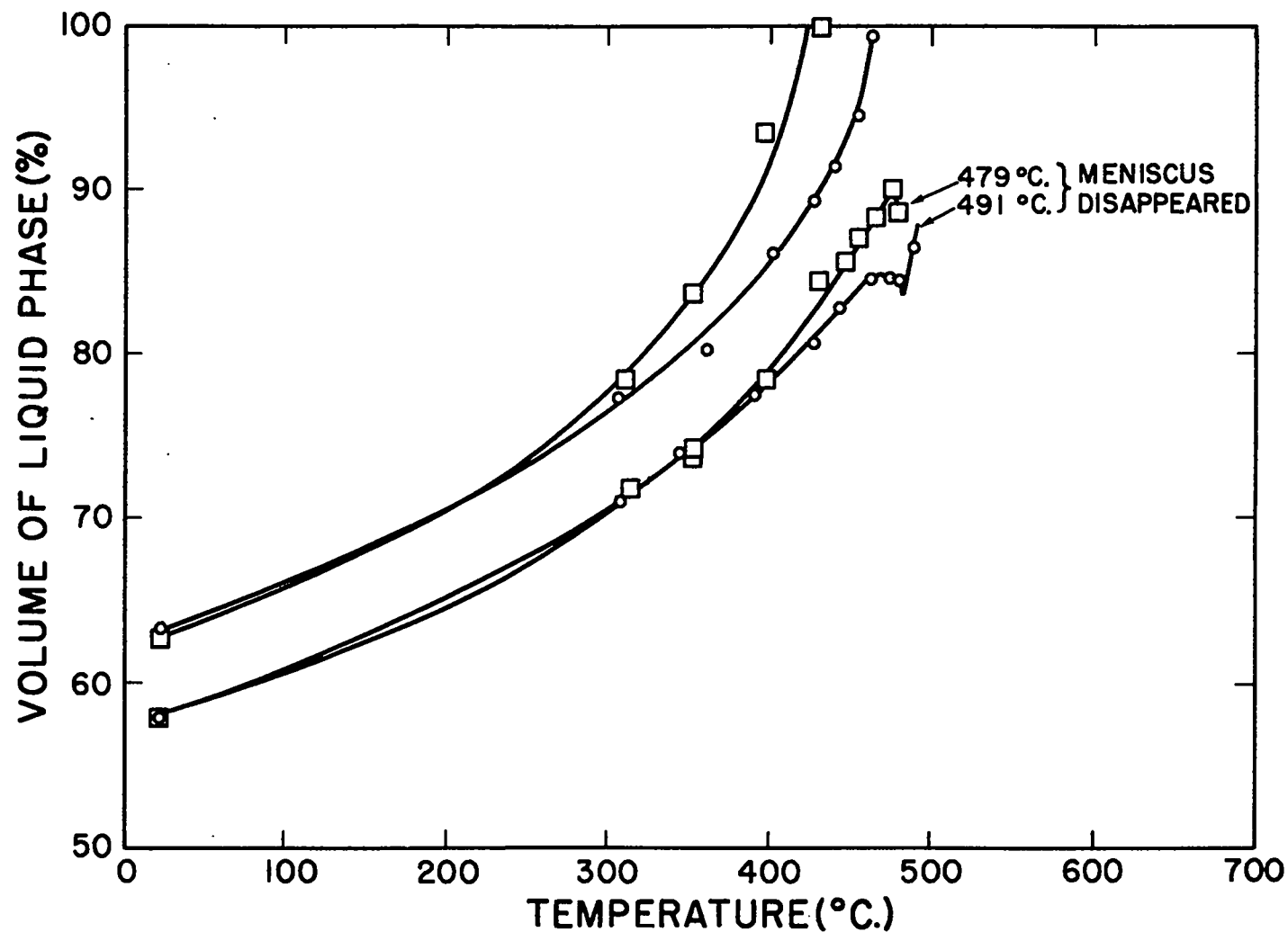


Fig. 1.7 Compressibility of Liquid Phase at Elevated Temperatures

□ - 0.46 M  $\text{UO}_3$  in 5.61 M  $\text{H}_3\text{PO}_4$  + initially air at 1 atm

○ - 0.45 M  $\text{UO}_3$  in 5.56 M  $\text{H}_3\text{PO}_4$  + initially 200 psi of oxygen

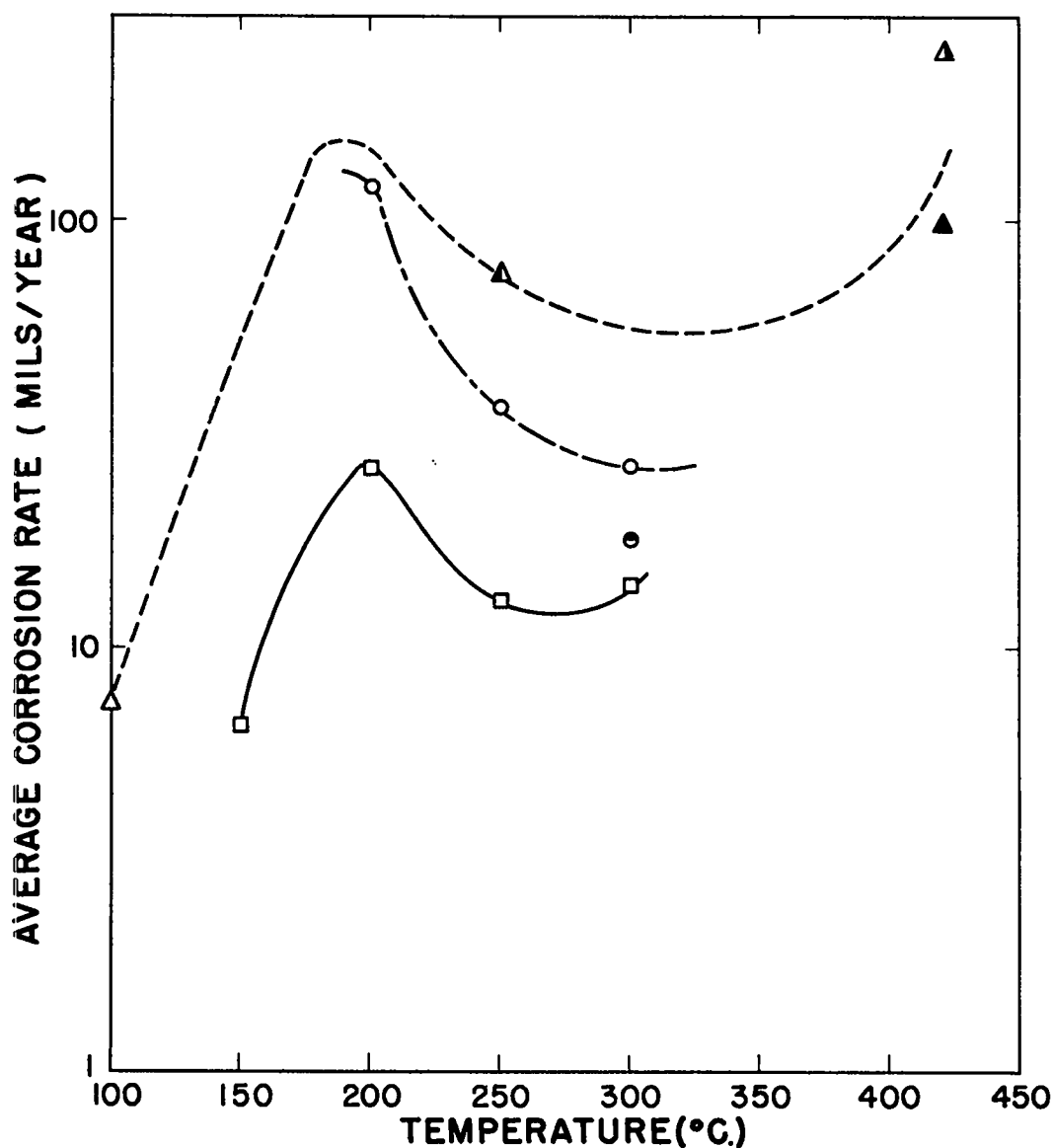


Fig. 1.8 The Corrosion Rate of Type 347 Stainless Steel vs. Temperature in  $H_3PO_4$  Solutions of  $UO_3$

- Δ - 0.5 M  $UO_3$  in 7.5 M  $H_3PO_4$ , 1 atm air, 14 days
- ▲ - 0.5 M  $UO_3$  + 0.001 M CuO in 7.5 M  $H_3PO_4$ , 100 psi (25° C.) of  $O_2$ , 4 days
- ▲ - 0.5 M  $UO_3$  + 0.002 M CuO in 7.5 M  $H_3PO_4$ , 100 psi (25° C.) of  $O_2$ , 4 days
- ▲ - 0.5 M  $UO_3$  in 7.5 M  $H_3PO_4$ , 100 psi (25° C.) of  $O_2$ , 4 days
- - 0.5 M  $UO_3$  + 0.001 M CuO in 5.2 M  $H_3PO_4$ , 100 psi (25° C.) of  $O_2$ , 4 days
- - 0.5 M  $UO_3$  + 0.001 M CuO in 5.2 M  $H_3PO_4$ , 200 psi (25° C.) of  $O_2$ , 4 days
- - 0.4 M  $UO_3$  in 3.0 M  $H_3PO_4$ , 1 atm (25° C.) of  $O_2$ , 4 days

increased rate at which the protective oxide coating is dissolved away. Above this temperature the corrosion rate decreases due to the formation of an adherent phosphate coating that impedes corrosion. The coating may cover the specimen uniformly at higher temperatures when the minimum in the curve is reached as, for example, with the 3 M phosphoric acid. However, in the series with 7.5 M phosphoric acid there was pitting of the specimen at temperatures corresponding to the corrosion minimum. With any concentration of phosphoric acid in Figure 1.8 there was again increased corrosion at still higher temperatures with progressively greater pitting. Generally, the higher the oxygen pressure the lower is the corrosion rate, as is illustrated by the extra point with double the oxygen pressure at 5.2 M  $\text{H}_3\text{PO}_4$ . The oxygen apparently helps in maintaining a protective coating. The lower curve of Figure 1.8 would indicate that moderately short-term use of 0.4 M  $\text{UO}_3$  in 3.0 M  $\text{H}_3\text{PO}_4$  contained in Type 347 stainless steel would be quite feasible at 250° to 300° C.

It has been shown by F. H. Beck and M. G. Fontana that the presence of  $\text{Cu}^{+2}$  above a certain concentration greatly inhibits the corrosion of stainless steels by 85% phosphoric acid at 130° C.<sup>14</sup> They found the critical concentration to produce corrosion inhibition to be in the range of 0.003 to 0.01 M  $\text{Cu}^{+2}$ . The amounts of dissolved  $\text{Cu}^{+2}$  present in the tests of Figure 1.8 were below this critical concentration, as the points at 420° C. would indicate. A difficulty is the limited solubility of cupric copper in solutions of  $\text{UO}_3$  in phosphoric

acid. The reason is the formation by copper and uranyl of a sparingly soluble double phosphate, the composition of which corresponds approximately to that of the mineral torbernite,  $\text{Cu}(\text{UO}_2\text{PO}_4)_2 \cdot 12\text{H}_2\text{O}$ . Table 1.4 gives some solubility values for  $\text{Cu}^{+2}$  in the presence of excess torbernite. It is considered impractical to have more copper present than is soluble at room temperature. However, a test at  $430^\circ \text{C}$ . with a solution of 1.0 M  $\text{UO}_3$  + 0.20 M  $\text{CuO}$  dissolved in 5.6 M  $\text{H}_3\text{PO}_4$  + 1.9 M  $\text{NaH}_2\text{PO}_4$  has been found to give pitting with Type 347 stainless steel. Hence, the use of this type stainless steel as a corrosion-resistant material in the presence of  $\text{Cu}^{+2}$  as a corrosion inhibitor has not seemed to be an answer to the problem, although further work probably would be justified.

Table 1.4

The Solubility of  $\text{Cu}^{+2}$  in Two  $\text{UO}_3$ - $\text{H}_3\text{PO}_4$  Solutions

Solution	Copper Molarity at $23^\circ \text{C}$ .	Copper Molarity at $430^\circ \text{C}$ .
1.0 M $\text{UO}_3$ in 5.5 M $\text{H}_3\text{PO}_4$	0.001	0.16
1.0 M $\text{UO}_3$ in 5.6 M $\text{H}_3\text{PO}_4$ + 1.9 M $\text{NaH}_2\text{PO}_4$	0.007	0.28

The use of sodium silicate or sodium chromate as a corrosion inhibitor for Type 347 stainless steel produced no improvement in resistance to corrosion. Spot checks with other types of stainless

steel such as 316 ELC, 317, and 310 showed them to be fairly similar to the 347 in corrosion resistance. The same could be said for the alloys Inconel, Inconel X, Nionel, the Hastelloys, and Haynes 25. Carpenter 20 stainless steel\* appeared to be significantly better than 347 stainless steel, as did zirconium and certain zirconium alloys such as Zr-1.7% Mo. In all of the foregoing tests chloride was present to the extent of about 0.1 ppm.

Either gold or platinum has been found to have a satisfactorily low corrosion rate at 430° C. or below, either with or without 10 ppm of added chloride. For example, gold at 430° C. in contact with a solution of 0.6 M UO<sub>3</sub> in 7.5 M H<sub>3</sub>PO<sub>4</sub> and 200 psi (25° C.) of oxygen gave a corrosion rate of 0.1 mil/year or less in the presence or absence of the added chloride. No pitting was observable under a microscope after such a test for four days. A method has been devised for detecting pinholes in gold plate or gold cladding that has been placed over a ferrous material of construction. The plated or clad object is immersed in an acidified 1% potassium ferricyanide solution and made anodic to a platinum cathode for 10 to 30 seconds. Ferrous ions are formed at the base of any pores existing in the gold and produce an insoluble blue compound with the ferricyanide that is not affected by subsequent washing of the specimen to remove acid. The location of any defects can be determined subsequently by visual inspection.

---

\* 20% Cr, 29% Ni, 1% Si, 0.07% C max., 2% Mo min., 3% Cu min.

Corrosion tests similar to the one with gold showed that corrosion rates of 0.1 mil/year or less were undergone by alloys such as 90% Pt-10% Ir, 90% Pt-10% Ru, 90% Pt-10% Rh, and 30% Pt-70% Au. Because of the partial conversion of gold to mercury that would take place in a reactor, similar tests were made with Hg-Au alloys. An alloy of 1% Hg-99% Au lost 90% of its mercury to the solution in two days. Hence, it is thought that no appreciable concentration of mercury could build up in the gold under these conditions. Of various precious metal solders that were tested, Incore 60 appeared to be the most satisfactory. It had a corrosion rate of about 30 mils/year.

## Chapter 2

### The System $\text{UO}_2\text{-H}_3\text{PO}_4\text{-H}_2\text{O}$

#### 2.1 Solubility

Determinations of uranium solubility were made in the same manner as in Section 1.1. The data are given in Table 2.1. The solid phase in each case was a uranous phosphate or pyrophosphate, of which three forms were observed above room temperature. They are described briefly in Table 2.2. Solid II appears to be the stable solid phase at the less elevated temperatures for concentrations of phosphoric acid of 9 M and higher. If that is true, then the uranium solubility actually may be less than indicated at 325° C. and lower temperatures for 16.3 to 16.5 M  $\text{H}_3\text{PO}_4$ . Table 2.3 contains the results of some measurements on the densities of some solutions of  $\text{UO}_2$  in  $\text{H}_3\text{PO}_4$ .

#### 2.2 Radiation Stability

The fact that solutions of  $\text{UO}_3$  in concentrated phosphoric acid spontaneously evolve oxygen to give uranous ion testifies to the great thermodynamic stability of the tetravalent state in such solutions. Hence, these solutions of  $\text{UO}_2$  would be expected to be stable in atmospheres that are reducing, inert, or moderately oxidizing. The upper curve of Figure 1.1 for such solutions as these is thought possibly to be too low due to certain experimental errors. Nevertheless, if a solution of enriched 0.5 M  $\text{UO}_2$  in 16.5 M  $\text{H}_3\text{PO}_4$  were exposed at 430° C. to a thermal neutron flux of  $10^{13}$ , the equilibrium pressure of radiolytic hydrogen and oxygen estimated from the figure would be less than 20 psi.



Table 2.1

Solubility Data in the System  $\text{UO}_2\text{-H}_3\text{PO}_4\text{-H}_2\text{O}$ 

Temperature, °C.	Analytical Molarities		Solid Phase
	U	Total Phosphate	
25	0.38 <sup>a</sup>	9.0	$\text{U}(\text{HPO}_4)_2 \cdot 6\text{H}_2\text{O}$
200	<u>ca.</u> 0.15	8.8	II
430	0.11	9.3	I
25	1.02 <sup>a</sup>	14.0	$\text{U}(\text{HPO}_4)(\text{H}_2\text{PO}_4)_2 \cdot \text{H}_2\text{O}$
370	0.30	14.0	III
430	0.24	14.0	III
175	0.51	16.3	III
250	0.67	16.5	III
325	0.55	16.3	III
370	0.46	16.6	III
430	0.42	16.5	III
490	0.44	16.6	III
174	0.43	17.6	II
250	0.48	17.6	II
326	$\geq$ 0.51	17.6	II
430	0.48	17.6	III
460	0.50	17.4	III

<sup>a</sup>Data at 25° C. have been taken from the report by J. M. Schreyer.<sup>15</sup>

Table 2.2

## Description of Solid Phases

- 
- Solid I: The crystals consisted of very small orthorhombic blades having a pale green color. The mean refringence was near 1.65. The composition was  $U(HPO_4)_2 \cdot H_2O$ .\*
- Solid II: The composition was  $U(HPO_4)(H_2PO_4)_2 \cdot 5H_2O$ .\*
- Solid III: Chemical analysis indicated a composition of  $U(HPO_4)_2$ .\* However, x-ray studies and studies of the optical properties of the crystals have led R. M. Douglass and E. Staritzky of this Laboratory to the conclusion that it was the orthorhombic  $UP_2O_7$  that has been observed previously.<sup>16</sup>
- 

\*The degree of hydration is uncertain by perhaps 1 molecule of water.

Table 2.3

The Density at 25° C. of Solutions of  $UO_2$  in  $H_3PO_4$ 


---

Solution Composition (molarities)	Density, g/ml at 25° C.
0.304 M $UO_2$ in 16.8 M $H_3PO_4$	1.8774
0.358 M $UO_2$ in 17.0 M $H_3PO_4$	1.8881
0.406 M $UO_2$ in 17.1 M $H_3PO_4$	1.9024
0.434 M $UO_2$ in 17.1 M $H_3PO_4$	1.9122
0.511 M $UO_2$ in 17.1 M $H_3PO_4$	1.9284

---

It is doubtful if any measurable oxidation of U(IV) would be produced under these conditions, particularly if a hydrogen overpressure were maintained as in LAPRE II.

### 2.3 Vapor Pressure

Figures 2.1 and 2.2 contain vapor-pressure data for solutions of 0.5 M  $\text{UO}_2$  dissolved in various concentrations of phosphoric acid. The initial degree of filling was 62% for each solution. The vapor pressures are at least a factor of 2 less than those of Figure 1.2 for the  $\text{UO}_3\text{-H}_3\text{PO}_4\text{-H}_2\text{O}$  system. As in the latter system, it is thought that the presence of dissolved  $\text{UO}_2$  in  $\text{H}_3\text{PO}_4$  would raise the vapor pressure to some extent. Figures 2.1 and 2.2 illustrate the marked reduction in vapor pressure that is obtainable in this range of  $\text{H}_3\text{PO}_4$  concentrations by increasing the concentration of acid. Judging from the data of E. H. Brown and C. D. Whitt, the vapor from even 100%  $\text{H}_3\text{PO}_4$  would consist mostly of water vapor.<sup>17</sup>

### 2.4 Thermal Expansion of the Liquid Phase

The measurements were made in the same manner as in Section 1.4. Representative data are shown in Figure 2.3. Because of the high concentrations of phosphoric acid, the critical temperatures probably would lie above 600° C., which is the maximum temperature that has been attained with the present transparent heating devices. The curves of Figure 2.3 are flatter than curves obtained at lower concentrations of phosphoric acid, thus lessening control-rod requirements in their application as reactor fuels at high temperatures.

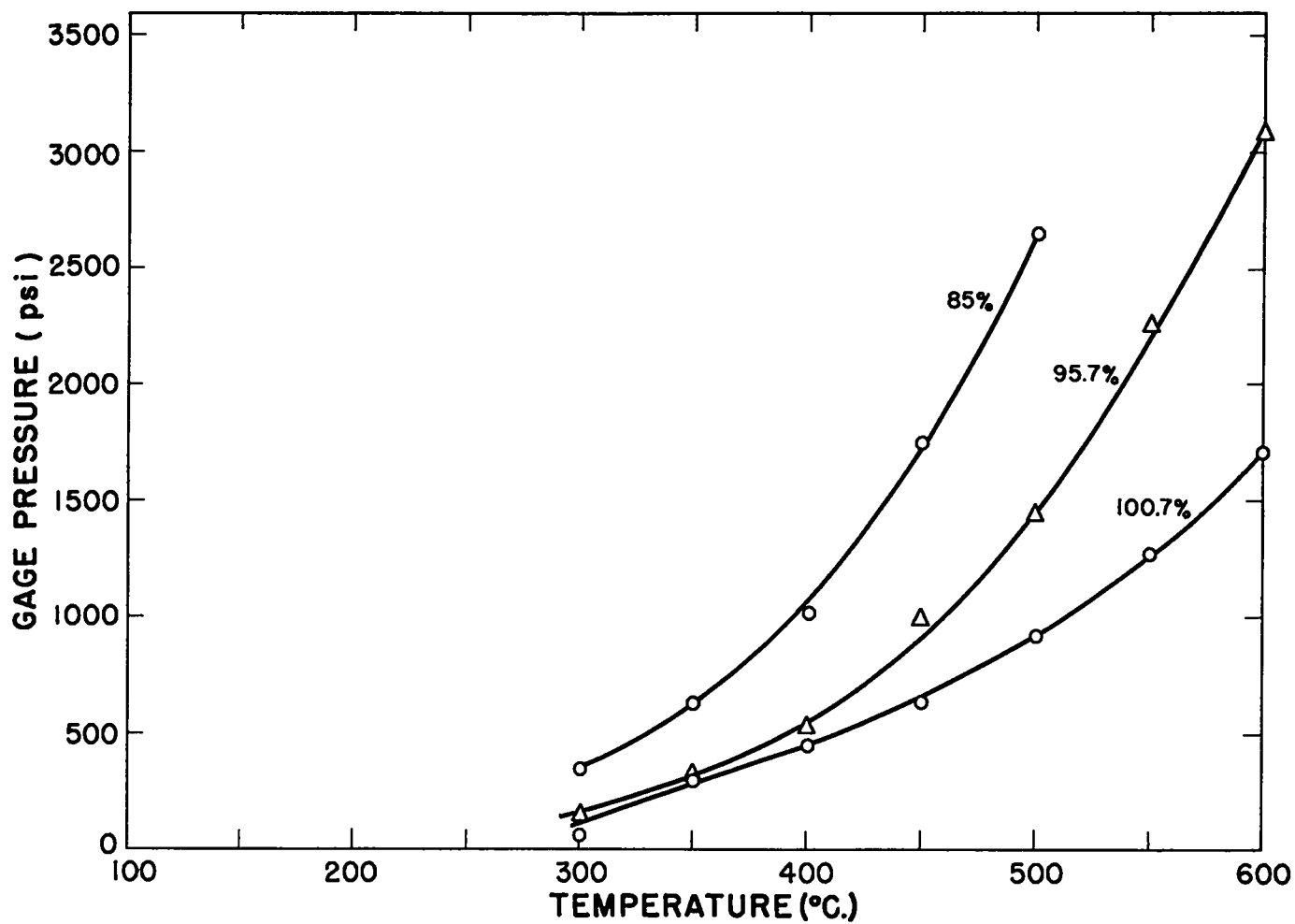


Fig. 2.1 Vapor Pressures vs. Temperature. 0.5 M Dissolved  $\text{UO}_2$ , 62% Initial Degree of Filling.

85% ~14.5 M  $\text{H}_3\text{PO}_4$

95.7% ~16.4 M  $\text{H}_3\text{PO}_4$

100.7% ~18.4 M  $\text{H}_3\text{PO}_4$

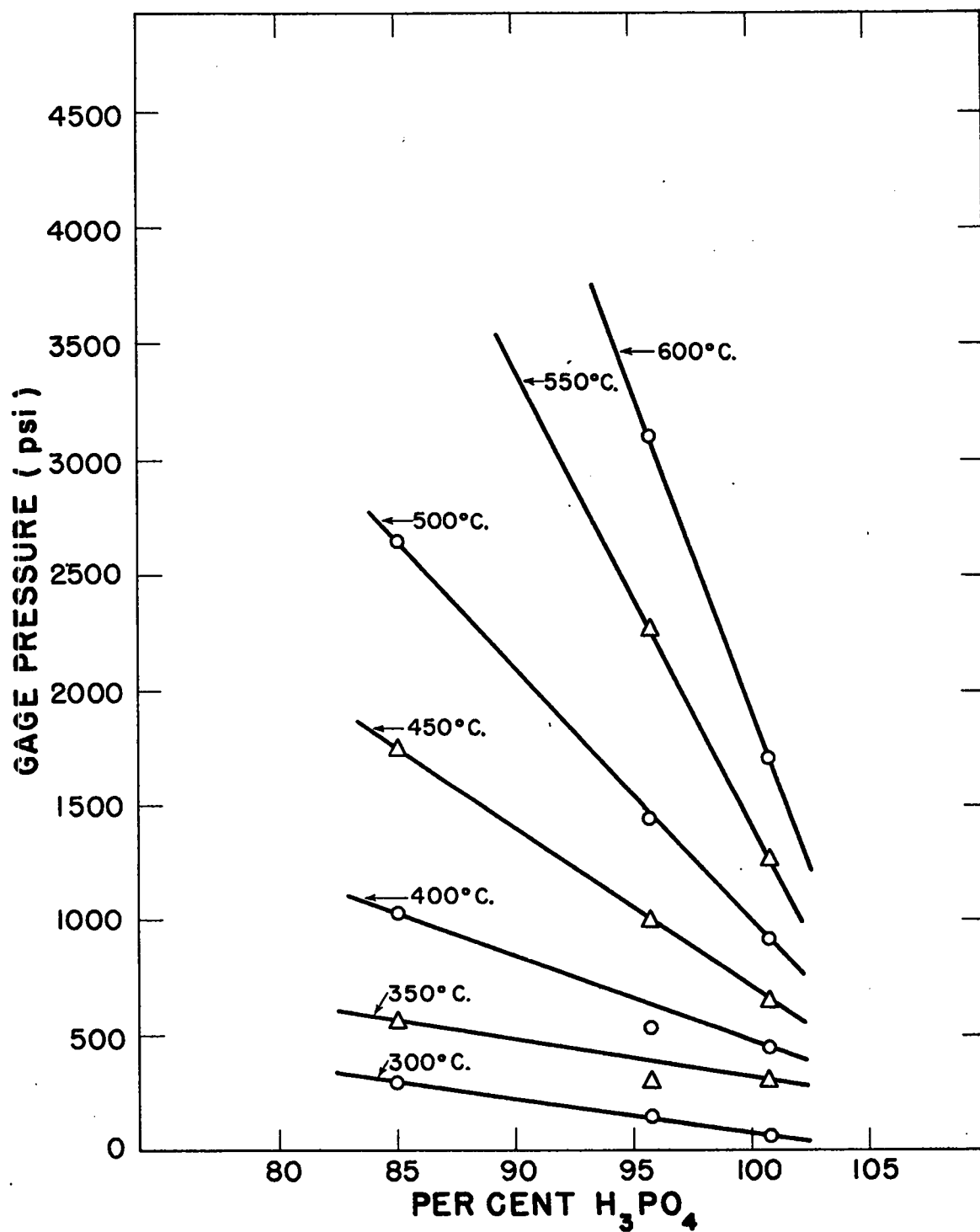


Fig. 2.2 Vapor Pressures vs.  $H_3PO_4$  Concentration. 0.5 M Dissolved  $UO_2$ , 62% Initial Degree of Filling.

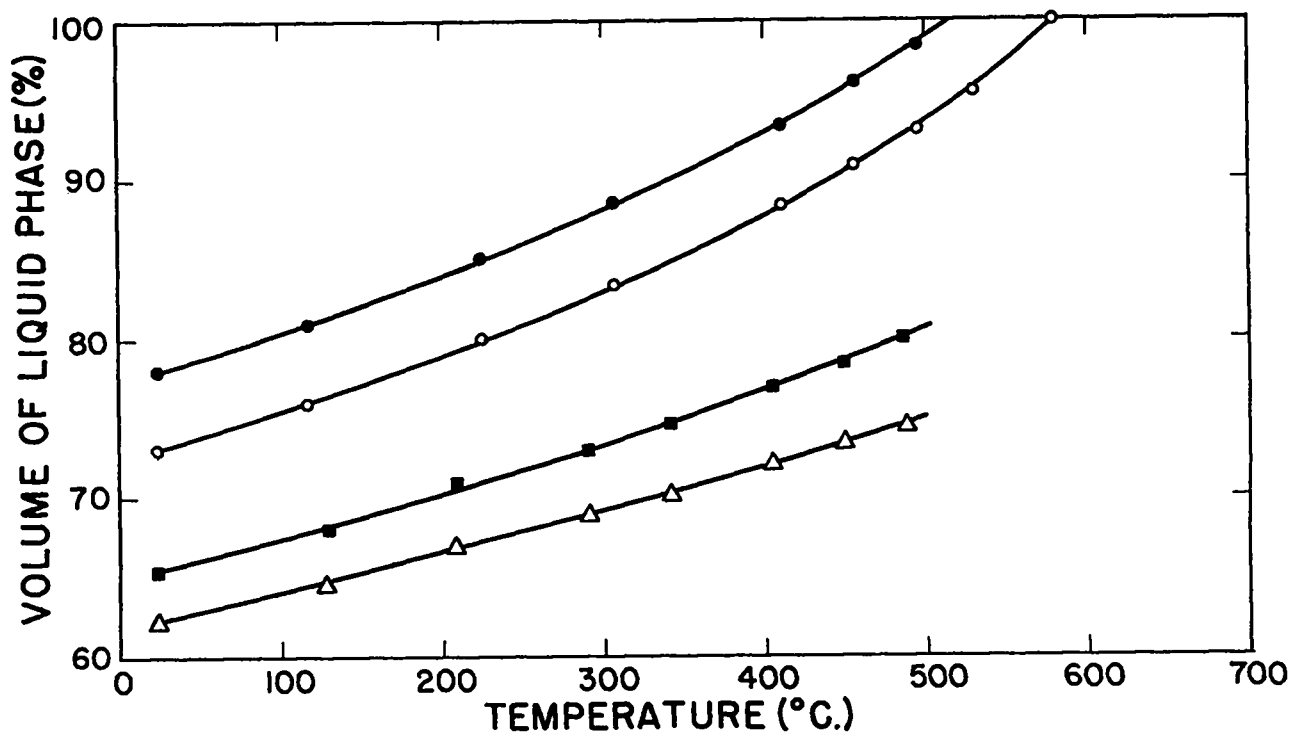


Fig. 2.3 Behavior of Liquid Volume vs. Temperature for Concentrated H<sub>3</sub>PO<sub>4</sub> Solutions

- - 0.40 M UO<sub>2</sub> in 14.1 M H<sub>3</sub>PO<sub>4</sub>
- - 0.34 M UO<sub>2</sub> in 15.5 M H<sub>3</sub>PO<sub>4</sub>
- - 0.36 M UO<sub>2</sub> in 16.2 M H<sub>3</sub>PO<sub>4</sub>
- △ - 0.4 M UO<sub>2</sub> in 18.1 M H<sub>3</sub>PO<sub>4</sub>

Characteristics other than thermal expansion may be observed on possible fuel solutions that have been sealed in thick-walled quartz (or Pyrex) capillaries. Observations of a semiquantitative nature may be made on solubilities in such solutions. For example, observations of this type currently are being made on condensed phosphoric acid solutions and solutions of  $\text{PuO}_2$ .

## 2.5 Corrosion

Gold and platinum are the only two metals that have been demonstrated to be completely corrosion-resistant above  $400^\circ\text{C}$ . to solutions of  $\text{UO}_2$  in concentrated phosphoric acid. The testing technique was the same as in Section 1.5.

The results obtained with gold were obtained at  $430^\circ\text{C}$ . with a solution of 0.4 M  $\text{UO}_2$  dissolved in 16.5 M  $\text{H}_3\text{PO}_4$ , which is a composition that might be representative of a LAPRE II type of solution. Corrosion rates of the order of the accuracy of detection (0.03 mil/year) or less were observed whether the gas phase above the solution was initially charged with air at 1 atm or 200 psi of hydrogen. These results were obtained whether the solution contained 0.2 ppm of chloride (from the reagents) or 10 ppm of chloride. Results obtained at  $430^\circ\text{C}$ . with  $\text{H}_4\text{P}_2\text{O}_7$ , pyrophosphoric acid, also indicated undetectable corrosion with similar atmospheres of air or hydrogen.

The use of gold as a cladding material in a reactor in which a high burn-up were to be used might result in the conversion of an appreciable fraction of the gold to mercury. For example, a thermal

neutron flux of  $10^{13}$  at the gold might give about 10% conversion to mercury in 1000 days of continuous operation. Since the Hg-Au alloy has a lower melting point than pure gold, its presence might restrict the reactor operation to lower temperatures unless the alloys so produced were dilute in mercury. Fortunately, mercury distills at an appreciable rate from even dilute Hg-Au alloys. This has been demonstrated with a 2% Hg-98% Au alloy immersed in a solution similar to the above having a similar hydrogen atmosphere. In four days at  $430^{\circ}$  C. the alloy lost one quarter of its mercury, of which one half was absorbed by a neighboring specimen of pure gold. There was no disruption of the surfaces caused by the migration of the mercury. This ease of movement of the mercury indicates that the gold cladding in the high-flux region of the reactor might lose part of its mercury to the comparatively large area of cladding that is in a much lower neutron flux. Other experiments under similar conditions indicate that mercury diffuses readily through a 15-mil gold lining and can be pumped off via grooves that have been cut in the wall proper. Therefore, during a reasonable life of the reactor, the resulting alloys should be dilute in mercury and should cause no trouble.

Silver and perhaps some other materials show promise below  $400^{\circ}$  C. as corrosion-resistant materials for solutions of  $\text{UO}_2$  in  $\text{H}_3\text{PO}_4$ . They are described in Appendix B.



## Chapter 3

### Reprocessing Methods

A solvent-extraction unit using tributyl phosphate has been developed by R. D. Baker, W. J. Maraman, and H. R. Baxman, of this Laboratory, for reprocessing spent reactor solutions such as that from LAPRE I. The properties of tributyl phosphate have been summarized in Volume 4 of The Reactor Handbook.<sup>18</sup> The nitric acid that necessarily accompanies the uranium in the solvent-extraction columns is to be removed from the product solution by boiling.

The uranium must be in the hexavalent state in this reprocessing method as well as in others shortly to be mentioned. Thus the uranium in spent fuel solutions from LAPRE II would first have to be converted to the hexavalent state before reprocessing and then reduced to the tetravalent state again before being returned to the reactor. Tetravalent uranium is oxidized automatically in concentrated nitrate solutions (as at the beginning of the above method). It also can be oxidized by the addition of 30%  $H_2O_2$  to concentrated phosphoric acid solutions. Reprocessed uranium in the hexavalent state may be converted to the tetravalent state in concentrated phosphoric acid solutions by the addition of hypophosphorous acid and heating at  $150^{\circ}C$ . for 1/2 hour. Preliminary experiments indicate also that 300 psi of hydrogen will reduce uranium to the tetravalent state in a matter of a few hours at  $200^{\circ}C$ .

In reprocessing an aqueous phosphate fuel solution one might use precipitations of uranyl ammonium phosphate (UAP).<sup>19</sup> However, additional work would be required to remove the ammonium ion from the reprocessed fuel solution before it was returned to the reactor. Similar considerations might apply for a uranyl sodium phosphate (USP) process.<sup>19</sup> Although these processes have disadvantages, they nevertheless might compare favorably with solvent-extraction methods in processing short-cooled fuel solutions because the inorganic reagents would be less subject to detrimental radiation damage than would organic reagents.

Spent  $\text{UO}_2\text{-H}_3\text{PO}_4$  fuel solutions might be processed to advantage in a method involving the precipitation of a double salt having a composition approximating that of the mineral torbernite  $\text{Cu}(\text{UO}_2\text{PO}_4)_2 \cdot 12\text{H}_2\text{O}$ . The solubility of U(VI) at 25° C. in a solution of 0.4 M  $\text{Cu}(\text{H}_2\text{PO}_4)_2$  + 0.2 M  $\text{H}_3\text{PO}_4$  is approximately  $1.1 \times 10^{-4}$  M. Decontamination factors have been observed to be about 7 for gamma activity and 4 for beta activity when torbernite is precipitated in 0.2 M  $\text{Cu}(\text{H}_2\text{PO}_4)_2$  + 0.1 M  $\text{H}_3\text{PO}_4$  containing fission-product activity that is 1 year old. The decontamination from fission-product poisons so obtained in one precipitation might be sufficient for returning the reprocessed fuel to the reactor. A more quantitative recovery of the uranium might be achieved with an additional precipitation of USP or UAP from the supernate from the torbernite precipitation followed by dissolution of the precipitate in sodium carbonate and recycling. The advantage of the use of the torbernite precipitation would be that the torbernite could readily be converted to a LAPRE II

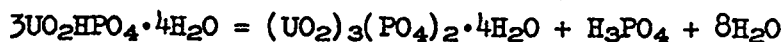
type of solution again. This step would be begun by dissolving the torbernite in phosphoric acid that contained some hypophosphorous acid [which would convert all of the copper to dissolved Cu(I)]. Then heating the solution would reduce all of the uranium to the desired tetravalent state and precipitate all of the copper as the metal.

## Appendix A

### The Effect on Uranium Solubility of Neutralizing Part of the $\text{H}_3\text{PO}_4$ or Substituting $\text{UO}_2(\text{NO}_3)_2$ for $\text{UO}_3$

The effect of increased pH on uranium solubility in phosphate solutions was studied by substituting  $\text{NaH}_2\text{PO}_4$  for part of the phosphoric acid. The data of Table A.1 were obtained with a solution having similar initial uranium and total phosphate concentrations as those of the solution used in obtaining the data of Table 1.1, but 15% of the total phosphoric acid had been neutralized to  $\text{NaH}_2\text{PO}_4$  in the case of the initial solution of Table A.1.<sup>6</sup> A comparison of the data of Tables A.1 and 1.1 indicates that a partial neutralization of the phosphoric acid leads to a slightly decreased uranium solubility.

The effect of decreased pH on uranium solubility was studied by substituting uranyl nitrate for the uranium trioxide dissolved in the phosphoric acid. The increased uranium solubility so obtained (Table A.2) as compared with the values of Table 1.1 shows the greater uranium solubility to be obtained by substituting  $\text{UO}_2(\text{NO}_3)_2$  for  $\text{UO}_3$  in phosphoric acid solutions. Two different solid phases were obtained by equilibrating the  $(\text{UO}_2)_3(\text{PO}_4)_2 \cdot 4\text{H}_2\text{O}$  with the 0.316 M  $\text{UO}_2(\text{NO}_3)_2$  in 2.07 M  $\text{H}_3\text{PO}_4$ . A solid phase obtained at 150° C. was  $\text{UO}_2\text{HPO}_4 \cdot 4\text{H}_2\text{O}$ . An optical examination by E. Staritzky, of this Laboratory, and chemical analyses (Table A.3) showed this solid to be essentially  $\text{UO}_2\text{HPO}_4 \cdot 4\text{H}_2\text{O}$  with a small amount of corrosion-product contaminants. The solid similarly obtained at 304° C. was found to be  $(\text{UO}_2)_3(\text{PO}_4)_2 \cdot 4\text{H}_2\text{O}$ . Hence, the transition



takes place at some temperature between 150° C. and 304° C., when the liquid phase is 0.3 M  $\text{UO}_2(\text{NO}_3)_2$  in 2 M  $\text{H}_3\text{PO}_4$ . G. R. Leader and J. W. Richter have obtained evidence indicating that the above transition takes place at about 60° C. in 1 M  $\text{HNO}_3$  and an unspecified, but probably smaller, concentration of phosphoric acid.<sup>20</sup> A similar transformation of  $\text{UO}_2\text{NH}_4\text{PO}_4 \cdot 3\text{H}_2\text{O}$  into  $(\text{UO}_2)_3(\text{PO}_4)_2 \cdot 4\text{H}_2\text{O}$  has been observed by A. D. Ryon and D. W. Kuhn to take place at about 80° C. in 0.8 to 1.6 M  $\text{HNO}_3$ .<sup>21</sup>

Table A.1

Solubility Data Obtained Upon Equilibrating Excess Solid  
 $(\text{UO}_2)_3(\text{PO}_4)_2 \cdot 4\text{H}_2\text{O}$  with a Solution of Initially 0.3 M  $\text{UO}_3$   
 Dissolved in 1.7 M  $\text{H}_3\text{PO}_4$  + 0.3 M  $\text{NaH}_2\text{PO}_4$   
 (Equilibrium Solid Phase:  $(\text{UO}_2)_3(\text{PO}_4)_2 \cdot 4\text{H}_2\text{O}$ )

Temperature, °C.	Analytical Molarities		Estimated Molalities	
	U	Total Phosphate	U	Total Phosphate
25	< 0.30 > 0.16	1.90	< 0.33 > 0.18	2.10
200	0.216	1.89	0.239	2.09
295	0.171	1.86	0.189	2.05
333	0.136	1.99	0.151	2.21
335	0.217	2.14	0.243	2.40
350	0.157	1.97	0.174	2.18

Table A.2

Solubility Data Obtained Upon Equilibrating Excess Solid  
 $(\text{UO}_2)_3(\text{PO}_4)_2 \cdot 4\text{H}_2\text{O}$  with a Solution of Initially  
 0.316 M  $\text{UO}_2(\text{NO}_3)_2$  Dissolved in 2.07 M  $\text{H}_3\text{PO}_4$

Temperature °C.	Analytical Molarities			Estimated Molalities		
	Uranium	Nitrate	Phosphate	Uranium	Nitrate	Phosphate
200	0.335	0.563	1.89	0.380	0.638	2.14
250	0.34 ± 0.02	0.65	2.00	0.39 ± 0.02	0.74	2.29
304	0.34 ± 0.02	0.65	2.00	0.39 ± 0.02	0.74	2.29

Table A.3

Composition of Solid Phase After Equilibrating  $(\text{UO}_2)_3(\text{PO}_4)_2 \cdot 4\text{H}_2\text{O}$   
 at 150° C. with Initially 0.316 M  $\text{UO}_2(\text{NO}_3)_2$  in 2.07 M  $\text{H}_3\text{PO}_4$

	Wt. % $\text{UO}_2^{+2}$	Wt. % $\text{PO}_4^{-3}$	Wt. % Fe + Cr
Sample No. 1	59.2	22.1	0.6
Sample No. 2	57.2	21.6	1.1
Theoretical for $\text{UO}_2\text{HPO}_4 \cdot 4\text{H}_2\text{O}$	61.6	21.7	---
Theoretical for $(\text{UO}_2)_3(\text{PO}_4)_2 \cdot 4\text{H}_2\text{O}$	75.6	17.7	---

## Appendix B

### The Corrosion Resistance of Various Materials in Solutions of $\text{UO}_2$ Dissolved in $\text{H}_3\text{PO}_4$

Silver and copper were found to have some corrosion resistance to concentrated phosphoric acid solutions if a neutral or reducing atmosphere was maintained. Hence, a little phosphorous acid,  $\text{H}_3\text{PO}_3$ , often was incorporated in the solutions to ensure the presence of a reducing atmosphere. The  $\text{H}_3\text{PO}_3$  would react at elevated temperatures with the oxygen of the air in the bomb as well as with any hexavalent uranium that was present with the dissolved  $\text{UO}_2$ . The excess  $\text{H}_3\text{PO}_3$  then would decompose to phosphoric acid, phosphorus, and hydrogen.

Some results obtained at low temperatures are shown in Table B.1. Except for the figure with the asterisk, the figures were obtained in the presence of air, the oxygen of which may not have been completely removed by reaction with the  $\text{H}_3\text{PO}_3$ . Under these conditions Type 347 stainless steel is a good container material, at least up to  $50^\circ\text{C}$ . The presence of hydrogen has an adverse effect on the corrosion rate of 347 stainless steel, possibly because hydrogen destroys its protective oxide film.

Table B.2 contains the results of some orienting experiments at  $430^\circ\text{C}$ . (In this and subsequent tables the initial degree of filling was 63%.) Of the bare specimens, silver was the best. Its corrosion rate did not vary markedly with the concentration of phosphoric acid.



Table B.1

Corrosion Tests with a Solution of 0.77 M  $\text{UO}_2$  + 0.03 M  $\text{UO}_3$   
Dissolved in 14.1 M  $\text{H}_3\text{PO}_4$  + 0.20 M  $\text{H}_3\text{PO}_3$

Specimen	Average Penetration Rate, mils/year		
	21 days at 23° C.	21 days at 50° C.	4 days at 100° C.
Copper	2.8	1.3	90 <sup>a</sup>
Silver	0.06	1.4	Not tested
347 stainless steel	0.01	0.01	1.0, 2.9 <sup>b</sup>

<sup>a</sup>The solution in this test was 0.38 M  $\text{UO}_2$  + 0.02 M  $\text{UO}_3$  in 16.5 M  $\text{H}_3\text{PO}_4$  containing no  $\text{H}_3\text{PO}_3$ .

<sup>b</sup>The higher figure was obtained with 1100 psi of hydrogen placed over the solution at room temperature instead of 1 atm of air.

Bare Everdur 1015 has about the same corrosion rate as bare copper, but the Everdur has considerably more structural strength. The protective action of the presence of graphite also is illustrated in the table. In these and subsequent tests the graphite did not appear to be attacked.

Gold plating had a beneficial effect on the corrosion of silver or copper, but the effect of diffusion into the gold was excessive in the case of copper. Table B.3 gives representative results at 430° C. Subsequent tests with plated specimens were made with plated silver. It had been shown that the presence of a stick of graphite exerted a protective action as did also the presence of an appreciable pressure of hydrogen. Although

Table B.2  
Corrosion Tests at 430° C. for Four Days,  
Each Solution Containing 0.20 M H<sub>3</sub>PO<sub>3</sub>

Specimen	Solution	Average Penetration Rate, mils/year
Bare silver	14.5 M H <sub>3</sub> PO <sub>4</sub>	67
Bare silver in contact with a stick of graphite	14.5 M H <sub>3</sub> PO <sub>4</sub>	5
Bare Everdur 1015 <sup>a</sup>	14.5 M H <sub>3</sub> PO <sub>4</sub>	432
Bare type 317 stainless steel	14.5 M H <sub>3</sub> PO <sub>4</sub>	> 2000
Bare silver	17.4 M H <sub>3</sub> PO <sub>4</sub>	80
Graphite-clad copper <sup>b</sup>	17.4 M H <sub>3</sub> PO <sub>4</sub>	16

<sup>a</sup>Alloy of 98.10% Cu, 1.65% Si, 0.29% Mn, and 0.05% Fe.

<sup>b</sup>The graphite cladding was 1/16" thick.

these effects were very marked with bare silver, they were ineffective in protecting silver within pinholes that had been drilled through gold plate which had been applied on silver. These conclusions are supported by the results of Table B.4. Pinholes of 5 mil diameter had been drilled through the gold plate into the silver before the corrosion runs were begun. The depth of the pinholes before and after each corrosion run was measured with a sharp-focus microscope to give the penetration produced by corrosion. Although the over-all sample corrosion rate was hardly

Table B.3  
Corrosion Tests at 430° C. for 25 Days  
in 14.5 M  $\text{H}_3\text{PO}_4$  + 0.20 M  $\text{H}_3\text{PO}_3$

Specimen	Av. Penetration Rate of Silver or Copper, mils/year	Appearance of Corroded Specimen
3 mils gold plate on silver	0.08	Unchanged except for a faintly lighter color of the gold
1 mil gold plate on copper	40	Copper-colored surface with eruptions through plate and corrosion beneath plate

measurable, the corrosion rate of silver within the pinholes was high.

Similar pinholes drilled in bare silver were found to give much less local corrosion if the silver was encased in graphite, as may be seen from the results shown in Table B.5. The over-all corrosion rate of the silver appeared to decrease as the silver-graphite clearance was increased to 60 mils.

In no corrosion test with silver or copper was there any insoluble silver or copper salt formed. Hence, the specimens had no adhering corrosion product. In an inert or reducing atmosphere the "corrosion" of either silver or copper was due mainly to mass transfer. The mass transfer often was evidenced by a silver or copper color having been produced on the platinum or gold lining of the bomb. The corrosion specimens

Table B.4

## Pinhole and Average Corrosion Rates with Gold-Plated Silver

Specimen	Solution	No. Days at 430° C.	Penetration in Pinhole, mils	Pinhole Corrosion Rate, mils/year	Over-all Sample Corrosion Rate, mils/year
3 mil Au/60 mil Ag/347 SS plus graphite stick	0.58 M UO <sub>2</sub> + 0.02 M UO <sub>3</sub> in 14.0 M H <sub>3</sub> PO <sub>4</sub> + 0.20 M H <sub>3</sub> PO <sub>3</sub>	14	3.0 ± 0.4	80	0.00 ± 0.04
Same	Same	28	5.5 ± 0.9	72	0.00 ± 0.02
Same	Same	42	12.3 ± 0.2	142	0.02 ± 0.01
3 mil Au/10 mil Ag/347 SS plus 200 psi H <sub>2</sub> (25° C.)	0.25 M UO <sub>2</sub> + 0.004 M UO <sub>3</sub> in 14.2 M H <sub>3</sub> PO <sub>4</sub>	14	3.0 ± 0.2	77	0.00 ± 0.04
Same	Same	29	4.0 ± 0.3	50	0.00 ± 0.02
Same	Same	42	8.4	73	0.0 ± 0.1

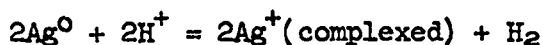
Table B.5

## Pinhole and Average Corrosion Rates with Graphite-Clad Silver

(Conditions: Nine Days at 430° C. with 0.58 M  $\text{UO}_2$  + 0.02 M  $\text{UO}_3$  in 14.0 M  $\text{H}_3\text{PO}_4$  + 0.20 M  $\text{H}_3\text{PO}_3$ )

Specimen	Penetration in Pinhole, mils	Pinhole Corrosion Rate, mils/year	Over-all Sample Corrosion Rate, mils/year
Unplated Ag encased in 1/8" graphite with 1 to 2 mils Ag-C clearance (on diam- eter)	0.05 ± 0.05	2 ± 2	0.30
Unplated Ag encased in 1/8" graphite with 30 mils Ag-C clearance (on diam- eter)	0.2 ± 0.1	8 ± 4	0.08
Unplated Ag encased in 1/8" graphite with 60 mils Ag-C clearance (on diam- eter)	0.0 ± 0.2	0 ± 8	0.07

always were located in the coolest portion of the bomb, which was about 10° C. cooler than the hottest portion. Specimens of silver that were corrosion-tested with part of the silver specimen projecting into the vapor phase were found to have comparatively negligible corrosion in the vapor phase. This indicates that the mechanism of mass transfer is not due to the vapor pressure of the metal. A more likely mechanism is via the equilibrium



which lies considerably to the left even at 430° C., but not so much so as to prevent mass transfer. The data of Table B.6 were obtained with various pressures of hydrogen, the presence of which should repress mass transfer according to the above equilibrium. The differences among the penetration rates for the first four entries may not be significant. A hydrogen pressure of 200 psi is practically as effective as a pressure of 1000 psi, which would indicate that the mass transfer at these hydrogen pressures probably is caused by another mechanism which is not understood. The last entry of the table indicates that 200 psi of hydrogen is comparatively ineffective in protecting copper.

A corrosion test like that of Table B.6 with silver and 200 psi of hydrogen was repeated with pinholes of 5 mils diameter drilled into the bare silver surface. The corrosion rate within the pinholes appeared to be no greater than on the surface, and that rate was about 10 mils per year. Another test like that in Table B.6 with 0.0015 M added  $\text{Na}_2\text{SiO}_3$  led to a threefold increase in corrosion.

Table B.6

The Effect of Hydrogen on the Corrosion of Bare Silver  
(Conditions: Four Days at 430° C. with 14.7 M H<sub>3</sub>PO<sub>4</sub>)

Bare Specimen	Hydrogen Pressure at 25° C., psi	Average Penetration Rate, mils/year
Silver	1000	6.6
Silver	300	8.1
Silver	200	6.5
Silver	100	10.1
Silver	40	70
Copper	200	300

Table B.7

Corrosion Tests in the Absence of Galvanic Couples  
(Conditions: 430° C. with 0.37 M UO<sub>2</sub> + 0.03 M UO<sub>3</sub> in 16.8 M H<sub>3</sub>PO<sub>4</sub> +  
0.10 M H<sub>3</sub>PO<sub>2</sub> and 200 psi of H<sub>2</sub> Initially Present at 25° C.)

Specimen	Time, days	Average Build-up of Metal on Specimen, mils
Silver	4	0.016
Silver	9	0.039
Copper	4	0.112

The results mentioned in the preceding paragraph and those shown in Tables B.4 and B.5 suggest that there may have been galvanic corrosion between the exposed silver and the gold areas including the gold cladding of the bomb. Thus the intensity of corrosion within the pinholes of Table B.4 was high because of the small area of silver that was exposed. The corrosion of the silver shown in Table B.5 was lessened because of the larger silver area and because of the Faraday Cage effect produced by the galvanically less harmful graphite. Also, the results of the preceding paragraph were obtained with a large silver area. The results of Table B.7 were obtained in the absence of galvanic couples by corrosion testing the silver in a silver-clad bomb and the copper in a copper-clad bomb. The specimens gained in weight, in each case due to mass transfer from the bomb wall, which may have been 5 or 10° C. warmer than the specimen.

Figure B.1 shows the effect of different temperatures on the corrosion of silver by 14.7 M  $\text{H}_3\text{PO}_4$ . The data indicate that above a certain temperature near the critical temperature of water the corrosion rate increases from about 1 mil/year at the rate of about 1 mil/year per 10° C. The increased corrosion rate might be due in part to the appearance of some pyrophosphoric acid at the higher temperatures. For example, 17.6 M  $\text{H}_3\text{PO}_4$  has been found to have about 5% of its phosphorus in the form of pyrophosphoric acid at 430° C.

The corrosion of bare silver at 430° C. in the presence of 200 psi (25° C.) of hydrogen is not affected appreciably by variations in



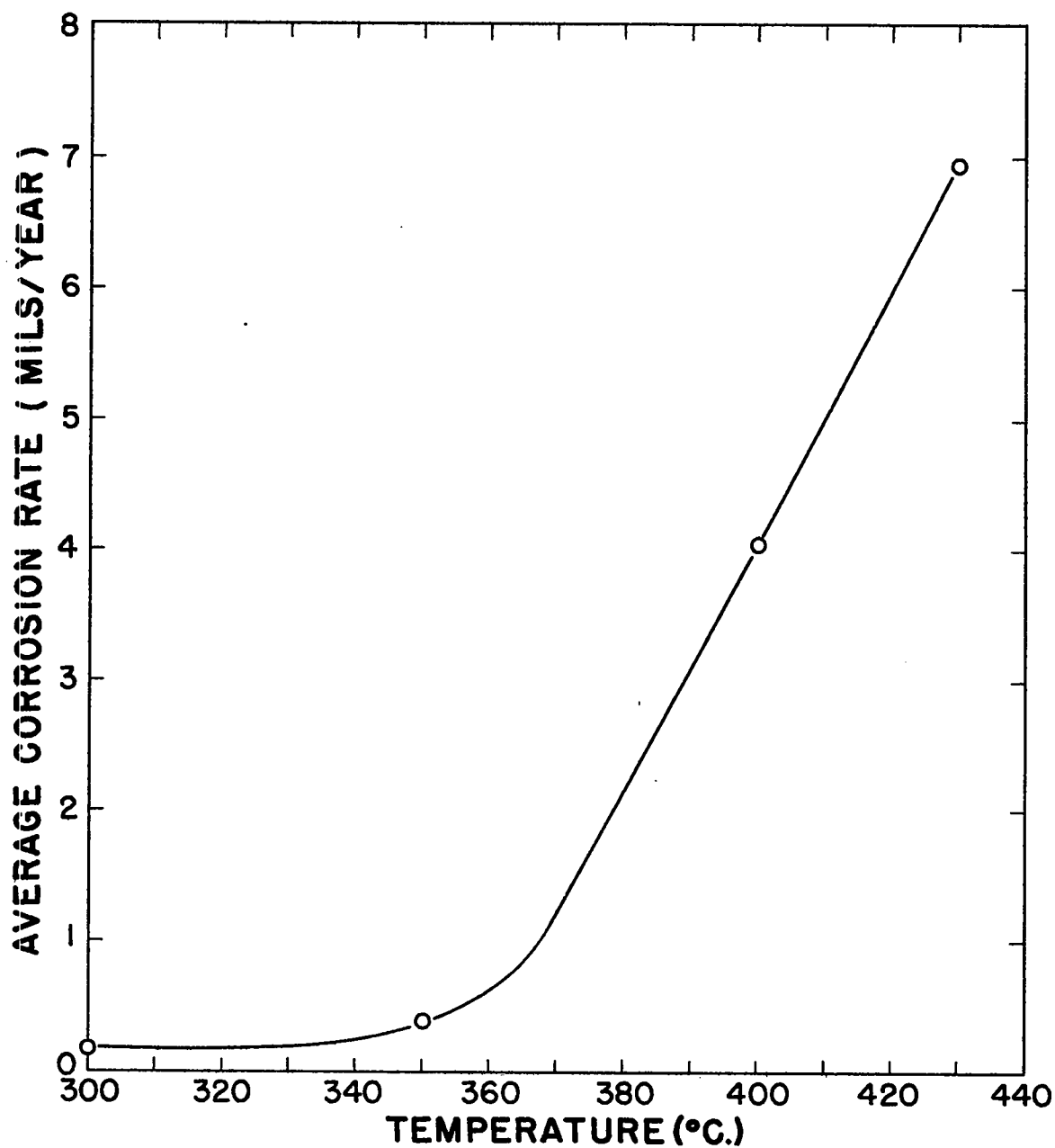


Fig. B.1 Corrosion Rate vs. Temperature for Bare Silver.  
[Conditions: 4 days in 14.7 M  $\text{H}_3\text{PO}_4$  with 200 psi  
(25° C.) of hydrogen.]

the phosphoric acid concentration in the range 9 to 17.6 M. The introduction of 0.4 M dissolved  $\text{UO}_2$  does not influence the corrosion rate at  $350^\circ \text{C.}$ , but it has been observed to increase the corrosion rate three-fold at  $430^\circ \text{C.}$

Tests have indicated that Incore 60 is a satisfactory solder for use in solutions of  $\text{UO}_2$  in  $\text{H}_3\text{PO}_4$ . Tests of a preliminary nature have indicated that tantalum as a corrosion-resistant material would be intermediate between silver and copper at  $430^\circ \text{C.}$  in agreement with a similar order of corrosion resistance observed by R. F. Miller, R. S. Treseder, and A. Wachter at  $250^\circ \text{C.}$ <sup>22</sup> Preliminary tests also show molybdenum to have some corrosion resistance.

## REFERENCES

1. R. M. Bidwell, W. R. Wykoff, and B. J. Thamer, "Filter-Bomb Sampling Technique for Phase Equilibria at Elevated Temperatures and Pressures," *Nucleonics* 14, <sup>No. 7,</sup> 166 (1956).
2. R. M. Bidwell, W. R. Wykoff, B. J. Thamer, and C. D. Ross, "Precious Metal Coated Bombs for High Temperature Phase and Irradiation Studies." To appear in *Nucleonics* in 1956.
3. W. W. Harris and R. H. Scott, "Optical Properties of Three Uranium Phosphates," Carbide and Carbon Chemicals Corporation Report K-508, Sept. 30, 1949.
4. B. J. Thamer, R. M. Bidwell, and R. P. Hammond, "The Solubility of Uranium in Possible Fuels for Homogeneous Reactors." Paper presented at Second Fluid Fuels Development Conference, Oak Ridge, April 17-18, 1952. Available in transcribed form in CF-52-4-197, Oak Ridge National Laboratory, p. 191.
5. E. Staritzky and D. I. Walker, "Optical Properties of Some Compounds of Uranium, Plutonium, and Related Elements," Report LA-1439, June 6, 1952, p. 31.
6. R. M. Bidwell, B. J. Thamer, and R. P. Hammond, Tables 4.3.61, 4.3.62, and 4.3.63 in The Reactor Handbook, Volume 2, Engineering, 1st ed., U. S. Atomic Energy Commission, Technical Information Service, RH-2, Sept., 1953.
7. O. H. Day, J. S. Gill, W. L. Marshall, and H. W. Wright, "The Uranium Trioxide-Orthophosphoric Acid-Water System," Chemistry Division Quarterly Progress Report for Period Ending June 30, 1951, Oak Ridge National Laboratory Report ORNL-1116, Feb. 14, 1952, p. 68.

8. W. L. Marshall et al., "The Uranium Trioxide-Phosphoric Acid-Water System," Homogeneous Reactor Project Quarterly Progress Report for Period Ending August 15, 1951, Oak Ridge National Laboratory Report ORNL-1121, Jan. 9, 1952, p. 119.
9. J. M. Schreyer and C. F. Baes, Jr., "The Chemistry of Uranium(VI) Orthophosphate Solutions: Part II, The Solubility of Uranium (VI) Orthophosphates in Phosphoric Acid Solutions," Oak Ridge National Laboratory Report ORNL-1578, June 30, 1953; J. Am. Chem. Soc. 76, 354 (1954).
10. T. A. Sims, "Final Status Report of the Fairchild NEPA Project," Report NEPA-1830, 1951, p. 149.
11. C. H. Secoy, "Survey of Homogeneous Reactor Chemical Problems." Paper presented at the Nuclear Engineering and Science Congress, Cleveland, Ohio, Dec. 12-16, 1955.
12. R. M. Bidwell and H. F. McDuffie, "Recombination and Reactor-Irradiation Behavior of Uranyl Phosphate-Phosphoric Acid Solutions," Oak Ridge National Laboratory Report CF-53-4-277, April 29, 1953.
13. J. H. Keenan and F. G. Keyes, Thermodynamic Properties of Steam Including Data for the Liquid and Solid Phases, John Wiley and Sons, Inc., New York, 1936.
14. F. H. Beck and M. G. Fontana, "Corrosion by Aqueous Solutions at Elevated Temperatures and Pressures," Corrosion 9, 287, 382 (1953).
15. J. M. Schreyer, "The Chemistry of Uranium(IV) Orthophosphate Solutions: Part I, The Solubility of Uranium(IV) Orthophosphates in Phosphoric Acid Solutions," Oak Ridge National Laboratory Report ORNL-1747, June 17, 1954.

16. A. Colani, *Ann. Chim. Phys.*, Series 8, Vol. 12, pp. 106, 115 (1907).
17. E. H. Brown and C. D. Whitt, "Vapor Pressure of Phosphoric Acids," *Ind. Eng. Chem.* 44, 615 (1952).
18. R. H. Long, A. E. Lindroos, and C. C. Randall, Chap. 2.3, p. 261, in The Reactor Handbook, Vol. 4, Fuel Reprocessing, 1st ed., U. S. Atomic Energy Commission, Technical Information Service, May, 1953.
19. R. H. Long and D. B. Stewart, Chap. 2.2, p. 69, in The Reactor Handbook, Vol. 4, Fuel Reprocessing, 1st ed., U. S. Atomic Energy Commission, Technical Information Service, May, 1953.
20. G. R. Leader and J. W. Richter, "Solubility of  $\text{BiPO}_4$  and Uranyl Phosphate in UNH Solutions," Clinton Laboratories Progress Report (Aug. 15, 1944 to Oct. 1, 1944) CN-2195, Dec. 26, 1944, pp. 19-24.
21. A. D. Ryon and D. W. Kuhn, "Solubility of Uranyl Ammonium Phosphate in Nitric Acid and Ammonium Nitrate Solutions as a Function of Temperature," Carbide and Carbon Chemicals Corporation Report Y-315, Jan. 10, 1948, p. 6.
22. R. F. Miller, R. S. Treseder, and A. Wachter, "Corrosion by Acids at High Temperatures," *Corrosion* 10, 7 (1954).